Surveys in Geophysics manuscript No.
(will be inserted by the editor)

The gravity anomaly of a 2D polygonal body having density contrast given by polynomial functions

M.G. D'Urso

Received: date / Accepted: date

Abstract An analytical solution is presented for the gravity anomaly produced by a 2D body whose geometrical shape is arbitrary and where the density contrast is a polynomial function in both the horizontal and vertical directions. Approximating the real shape of the body by a polygon, the solution is expressed as sum of algebraic quantities which depend only upon the coordinates of the vertices of the polygon and upon the polynomial density function. The solution presented in the paper, which refers to a third-order polynomial function as a maximum, exhibits an intrinsic symmetry which naturally suggests its extension to the case of higher-order polynomials describing the density contrast. Furthermore, the gravity anomaly is evaluated at an arbitrary point which does not necessarily coincides with the origin of the reference frame in which the density function is assigned. Invoking recent results of potential theory, the solution derived in the paper is shown to be singularity-free and numerically robust. The accuracy and effectiveness of the proposed approach is witnessed by the numerical comparisons with examples derived from the existing literature.

Keywords Gravity anomaly · 2D bodies · polynomial density contrast · Singularity

1 Introduction

The gravity anomaly of a region represents a basic set of geophysical data for the investigation of the subsurface density both in forward modelling and inversion (Jacoby and Smilde, 2009). For this reason it is highly beneficial to dispose of analytical solutions of the gravity anomaly associated with a body characterized by complex density distributions. Due to the mathematical complexity of the problem, the gravity anomaly of an irregular body whose density contrast is spatially variable has been first computed by approximating the body as a collection of vertical rectangular parallelepipeds (prisms) in which the density is assumed to be constant. Hence, the gravity anomaly for the whole body is computed as algebraic sum of the contribution of all vertical prisms at appropriate depths and distances from the observation point.

M.G. D'Urso
DICeM - Università di Cassino e del Lazio Meridionale
via G. Di Biasio 43, 03043 Cassino (FR), Italy
E-mail: durso@unicas.it

Numerical computations were first carried out by Talwani et al (1959) and Bott (1960). Closed form expressions of the gravity anomaly were subsequently derived by Nagy (1966), Banerjee and DasGupta (1977), Cady (1980), Nagy et al (2000), Tsoulis (2000), Jiancheng and Wenbin (2010), D'Urso (2012), see also Plouff (1975, 1976), Won and Bevis (1987), Montana et al (1992) for computer codes. The case of spheroidal shell has been addressed by Johnson and Litehiser (1972). Analytical expressions of the gravity anomaly for prisms have been derived by D'Urso (2015b), for a linearly varying density, by Rao (1985, 1986, 1990), Rao et al (1994), Gallardo-Delgado et al (2003) for a quadratic density contrast, by García-Abdeslem (1992, 2005a), when the density varies with depth according to a cubic law. Non-polynomial density-contrast models have been considered by Cordell (1973), Chai and Hinze (1988), Litinsky (1989), Silva et al (2006), Chappell and Kusznir (2008),. For more complicated forms of the density contrast, see, e.g., Cai and Wang (2005) and Mostafa (2008).

The previous contributions are characterized by simple geometric modelling, i.e. the use of prisms, and refined modelling of the density contrast. A different approach is based on the use of polyhedra, to avoid the necessity of subdividing the region of interest in several prisms, countervailed by a simple description of density contrast. Analytical formulas for the gravimetric analysis of polyhedra having constant density have been contributed by Paul (1974), Barnett (1976), Strakhov (1978), Waldvogel (1979), Golizdra (1981), Strakhov et al (1986), Pohanka (1988), Kwok (1991b), Werner (1994), Holstein and Ketteridge (1996), Petrović (1996), Werner and Scheeres (1997), Li and Chouteau (1998), Tsoulis (2012), D'Urso (2013a). Subsequent advancements have been only concerned with a linear density variation, (Pohanka, 1998; Hansen, 1999; Holstein, 2003; Hamayun et al, 2009; D'Urso, 2014b); actually, handling more complex density functions in conjunction with polyhedral models considerably increases the difficulties of the treatment, especially if analytical solutions are looked for.

As a matter of fact the interest in modelling gravity data using non-uniform density contrast is associated with the geological and economic relevance of sedimentary basins. Actually, the sediment thickness and bedrock topography are important parameters in modelling groundwater flow, petroleum exploration, geotectonic investigations and ground motion amplification during an earthquake (Jacoby and Smilde, 2009; Aydemir et al, 2014). The geologic evaluation of sedimentary basins can be quite complex so that the kind of function describing the density contrast significantly differs from case to case. For instance, if simple differential compaction is assumed to be the main diagenetic process in the evaluation of a sedimentary basin, geologically meaningful results are obtained by using an exponentially increasing density with depth. However, if more complex geological process come into play, such as nonuniform stratigraphic layering, facies changes etc., more general variations of density need to be taken into account.

Independently from the kind of function assumed to define the density contrast, density can be assumed to vary, separately or jointly, along the vertical and horizontal directions. For instance, variations of density can be either arbitrary in the horizontal direction and of polynomial type in the vertical one, or with an interchanged functional dependence. This last case does occur in dipping layered intrusions or sedimentary beds in which an arbitrary density function is assumed along depth and a polynomial function is considered in the horizontal direction. Furthermore, complicated density functions can be associated with 3D modelling based on prisms, (Murthy and Rao, 1979; Rao et al, 1990; Chakravarthi et al, 2002; Chakravarthi and Sundararajan, 2007; Zhou, 2009b), or with 2D geometrical shapes, (Gendzwill, 1970; Murthy and Rao, 1979; Pan, 1989; Guspí, 1990; Ruotoistenmäki, 1992; Martín-Atienza and García-Abdeslem, 1999; Zhang et al, 2001; Zhou, 2008, 2009a, 2010).

Actually, this last geometrical assumption, which characterizes domains having a cylindrical shape, significantly simplifies the mathematical treatment of the problem.

The derivation of analytical expressions for the gravity anomaly has not yet been achieved, even in presence of two-dimensional domains, for bodies characterized by a complicated density contrast, so that numerical methods have been resorted to. Specifically, starting from the first researches on the subject (Hubbert, 1948), all authors have systematically transformed the original domain integrals into integrals of lower dimension in order to simplify the adoption of quadrature rules for the numerical evaluation of the gravity anomaly.

For 2D bodies, which are the object of the present paper, Zhou (2008) converted the original domain integral for gravity anomaly to a Line Integral (LI) by using Stokes theorem. In particular he derived two types of LIs for computing the gravity anomaly of bodies having density contrast depending only on depth. In a subsequent paper (Zhou, 2009a) the author extended his method to account for density contrast functions which depended not only on depth but also on horizontal or, jointly, on horizontal and vertical directions. The original approach by Zhou has been further improved in Zhou (2010) to evaluate the gravity anomaly at observation points different from the origin since, historically, gravity anomaly was computed only at the origin of the reference frame. Furthermore, Zhou dealt with the singularity of the gravity anomaly arising where the observation point is coincident with the vertices of the integration domain, an issue already discussed in Kwok (1991a), for prism-based modelling, and Tsoulis and Petrović (2001) for polyhedra.

Aim of this paper is to derive an analytical expression of the gravity anomaly for polygonal bodies whose density contrast is expressed as a polynomial function of arbitrary degree in both the horizontal and vertical directions. The result is obtained by reducing the original domain integral to a boundary integral by virtue of the generalized Gauss theorem first presented in D'Urso (2012, 2013a), and subsequently applied to several problems ranging from geodesy, (D'Urso, 2014a,b, 2015b; D'Urso and Trotta, 2015c), to geomechanics, (Sessa and D'Urso, 2013; D'Urso and Marmo, 2015a; Marmo and Rosati, 2015), to geophysics (D'Urso and Marmo, 2013b) and to heat transfer (Rosati and Marmo, 2014). The generalized Gauss theorem referred to above does allow one not only to derive an expression of the gravity anomaly which is expressed in terms of a boundary integral but also to prove that the singularity of the gravity anomaly, arising when the observation point does belong to the integration domain, is eliminable.

For a polygonal domain Ω of n sides the expression of the gravity anomaly in terms of boundary integral is further specialized to the sum of n 1D integrals. Differently from previous contributions on the subject, such 1D integrals are not numerically evaluated but expressed analytically as a function of the position vectors defining the vertices of the integration domain and of scalar quantities I_{ki} defined on each side. In turn the quantities I_{ki}, pertaining to i-th edge of the boundary of Ω, are analytically computed by evaluating an integral of real variable which can exhibit a singularity when the edge does belong to a line containing the observation point. However, it is proved that such a singularity produces a null contribution of the i-th edge to the general expression of gravity anomaly; hence, one can conclude that the derived expression is singularity-free.

By exploiting a suitable change of variables, we also derive an enhanced algebraic formula which expresses the gravity anomaly at an arbitrary point P and specializes to the ordinary one when $P = O$. Remarkably, the enhanced expression of the gravity anomaly has been derived without any modification of the density contrast function since this is still defined in the original reference frame. The enhanced formula has been implemented in a Matlab code and its accuracy and robustness has been assessed by numerical comparisons with examples derived from the literature.

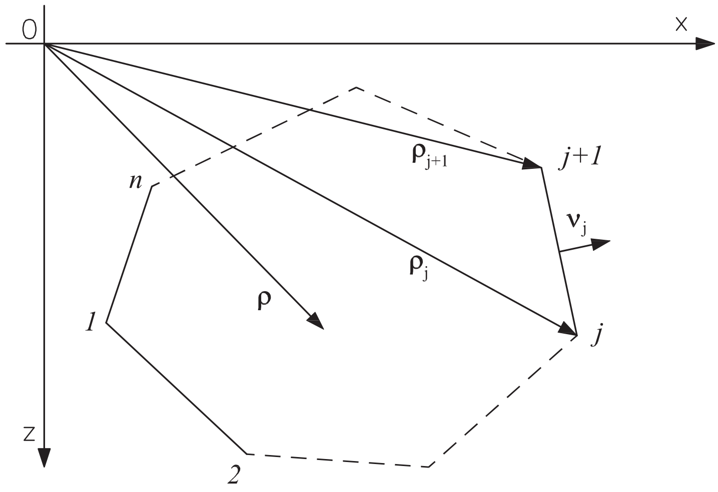

Fig. 1 Polygonal domain Ω and geometric quantities of the i-th edge

2 Gravity anomaly of a 2D body at the origin O of the reference frame

It is well known that the gravitation exerted by a 3D body $\hat{\Omega}$ on a unit mass at O is given by

$$\mathbf{g}(O) = G \int_{\hat{\Omega}} \frac{\Delta\rho(\mathbf{r})\,\mathbf{r}}{(\mathbf{r}\cdot\mathbf{r})^{3/2}} dV \tag{1}$$

where G is the gravitational constant, $\mathbf{r}$ the position vector pointing from O to an arbitrary point of $\hat{\Omega}$ and $\Delta\rho(\mathbf{r})$ the density contrast at $\mathbf{r}$. Hence, $\Delta\rho(\mathbf{r})dV(\mathbf{r})$ represents the infinitesimal difference between the mass at $\mathbf{r}$ and the background. We are interested to two-dimensional problems so that we shall denote by Ω the section of $\hat{\Omega}$ in the vertical plane and consider the reference frame sketched in fig. 1.

The vertical component $\mathbf{g}_z$ of gravitation at O is given by

$$\mathbf{g}_z(O) = G \int_{\hat{\Omega}} \frac{\Delta\rho(\mathbf{r})\mathbf{r}\cdot\mathbf{k}}{(\mathbf{r}\cdot\mathbf{r})^{3/2}} dV \tag{2}$$

where $\mathbf{k}$ is the unit vector directed downwards. Being $\hat{\Omega}$ infinite in the y-direction and assuming that the density contrast $\Delta\rho$ is independent from y, the previous integration can be carried out between two symmetric ordinates $\pm d_y$, with $d_y \to \infty$. Accordingly, one obtains

$$\mathbf{g}_z(0,0) = G \int_{\Omega} \Big[\lim_{d_y\to\infty} \int_{-d_y}^{d_y} \frac{\Delta\rho(x,z)\mathbf{r}\cdot\mathbf{k}}{(\mathbf{r}\cdot\mathbf{r})^{3/2}} dy\Big] dxdz = \int_{\Omega} \frac{\Delta\rho(x,z)z}{x^2+z^2} dA \tag{3}$$

This the general form of the 2D integral for calculating the gravity anomaly at O produced by a distribution of 2D masses having a density contrast $\Delta\rho$ with respect to the background. Actually, the gravity anomaly is defined as the line integral of the components of the 2D vector gravitation along the boundary of a mass body.

The computation of the integral in (3) is complicated by the fact that, due to geological and geochemical processes, the density contrast distribution within Ω can be arbitrary. A quite general expression for $\Delta\rho$, able to accommodate a large variety of geological formations, is given by a double polynomial in x and z, (Zhang et al, 2001; Zhou, 2008, 2009a, 2010)

$$\Delta\rho(x,z) = \theta(x,z) = \sum_{i=0}^{N_x} \sum_{j=0}^{N_z} c_{ij} x^i z^j \tag{4}$$

where N_x and N_z represent the maximum power of the polynomial density variation along x and z respectively.

The scalars c_{ij} represent the coefficients of the polynomial law; they can be estimated from the known data points by a least-square approach (Jacoby and Smilde (2009)). In the sequel we shall confine the treatment to case

$$N_x + N_z = 3 \tag{5}$$

since this will suffice to address the majority of the numerical examples previously considered in the literature and, at the same time, to present our formulation at a degree of generality sufficient to be generalized to the cases $N_x + N_z > 3$.

To simplify the ensuing developments it is convenient to introduce the two-dimensional vectors $\boldsymbol{\rho} = (x,z)$ and $\boldsymbol{\kappa}_z(0,1)$. In this way the previous relation can be written as

$$\mathbf{g}_z(\boldsymbol{o}) = 2G \int_{\Omega} \frac{\theta(\boldsymbol{\rho})(\boldsymbol{\rho}\cdot\boldsymbol{\kappa}_z)}{\boldsymbol{\rho}\cdot\boldsymbol{\rho}} dA \tag{6}$$

and our objective is to prove that the previous integral can be expressed as a line integral extended to the boundary $\partial\Omega$ of Ω. Paralleling an analogous treatment developed in D'Urso and Marmo (2013b), we first reformulate the general expression (4) of the density contrast by writing

$$\theta(\boldsymbol{\rho}) = \theta_{\boldsymbol{o}} + \mathbf{c}\cdot\boldsymbol{\rho} + \mathbf{C}\cdot\mathbf{D}_{\rho\rho} + \mathbb{C}\cdot\mathbb{D}_{\rho\rho\rho} \tag{7}$$

where $\theta_{\boldsymbol{o}}$ is a scalar, $\mathbf{c}$ is a vector, $\mathbf{C}$ and $\mathbf{D}_{\rho\rho}$ are symmetric second-order tensors, $\mathbb{C}$ and $\mathbb{D}_{\rho\rho\rho}$ are third-order tensors; furthermore, it has been set

$$\mathbf{D}_{\rho\rho} = \boldsymbol{\rho}\otimes\boldsymbol{\rho} \qquad \mathbb{D}_{\rho\rho\rho} = \boldsymbol{\rho}\otimes\boldsymbol{\rho}\otimes\boldsymbol{\rho} \tag{8}$$

The second-order (rank-two) tensor $\boldsymbol{\rho}\otimes\boldsymbol{\rho}$ has the following matrix representation

$$[\boldsymbol{\rho}\otimes\boldsymbol{\rho}] = \begin{bmatrix} x^2 & xz \\ xz & z^2 \end{bmatrix} \tag{9}$$

so that, being:

$$\mathbf{C}\cdot(\boldsymbol{\rho}\otimes\boldsymbol{\rho}) = C_{11}x^2 + 2C_{12}xz + C_{22}z^2 \tag{10}$$

a quadratic distribution of density can be assigned by suitably defining the coefficients of the symmetric tensor $\mathbf{C}$. Analogously, the third-order tensors $\mathbb{C}$ and $\boldsymbol{\rho}\otimes\boldsymbol{\rho}\otimes\boldsymbol{\rho}$, are represented in matrix form as:

$$\mathbb{C} = \left[\begin{array}{cc} \mathbb{C}_{111} & \mathbb{C}_{112} \\ \mathbb{C}_{121} & \mathbb{C}_{122} \\ \hdashline \mathbb{C}_{211} & \mathbb{C}_{212} \\ \mathbb{C}_{221} & \mathbb{C}_{222} \end{array}\right] \qquad \boldsymbol{\rho}\otimes(\boldsymbol{\rho}\otimes\boldsymbol{\rho}) = \left[\begin{array}{c} x\begin{bmatrix} x^2 & xz \\ xz & z^2 \end{bmatrix} \\ \hdashline z\begin{bmatrix} x^2 & xz \\ xz & z^2 \end{bmatrix} \end{array}\right] \tag{11}$$

i.e. as vectors of rank-two tensors. Being

$$\begin{aligned} \mathbb{C}\cdot(\boldsymbol{\rho}\otimes\boldsymbol{\rho}\otimes\boldsymbol{\rho}) &= \mathbb{C}_{111}x^3+(\mathbb{C}_{112}+\mathbb{C}_{121}+\mathbb{C}_{211})x^2z+ \\ &+(\mathbb{C}_{122}+\mathbb{C}_{212}+\mathbb{C}_{221})xz^2+\mathbb{C}_{222}z^3 \end{aligned} \tag{12}$$

the representation (4) of the density contrast is recovered from (7) by setting

$$\begin{aligned} \theta_{\boldsymbol{o}} &= c_{00} \qquad c_1 = c_{10} \qquad c_2 = c_{01} \\ C_{11} &= c_{20} \qquad C_{22} = c_{02} \qquad C_{12} = c_{11}/2 \end{aligned} \tag{13}$$

and

$$\mathbb{C}_{111} = c_{30} \qquad \mathbb{C}_{222} = c_{03} \tag{14}$$

$$\mathbb{C}_{112} = \mathbb{C}_{121} = \mathbb{C}_{211} = c_{21}/3 \qquad \mathbb{C}_{122} = \mathbb{C}_{212} = \mathbb{C}_{221} = c_{12}/3 \tag{15}$$

In conclusion, we derive from (6) the following expression of the gravity anomaly

$$\mathbf{g}_z(\boldsymbol{o}) = 2G\Big[\theta_{\boldsymbol{o}} d^{\Omega}_{\boldsymbol{\rho}} + \mathbf{c}\cdot\mathbf{d}^{\Omega}_{\boldsymbol{\rho}} + \mathbf{C}\cdot\mathbf{D}^{\Omega}_{\boldsymbol{\rho\rho}} + \mathbb{C}\cdot\mathbb{D}^{\Omega}_{\boldsymbol{\rho\rho\rho}}\Big] \tag{16}$$

where

$$d^{\Omega}_{\boldsymbol{\rho}} = \int_{\Omega} \frac{\boldsymbol{\rho}\cdot\boldsymbol{\kappa}_z}{\boldsymbol{\rho}\cdot\boldsymbol{\rho}}dA \qquad \mathbf{d}^{\Omega}_{\boldsymbol{\rho}} = \int_{\Omega} \frac{(\boldsymbol{\rho}\cdot\boldsymbol{\kappa}_z)\boldsymbol{\rho}}{\boldsymbol{\rho}\cdot\boldsymbol{\rho}}dA \tag{17}$$

and

$$\mathbf{D}^{\Omega}_{\boldsymbol{\rho\rho}} = \int_{\Omega} \frac{(\boldsymbol{\rho}\cdot\boldsymbol{\kappa}_z)\boldsymbol{\rho}\otimes\boldsymbol{\rho}}{\boldsymbol{\rho}\cdot\boldsymbol{\rho}}dA \qquad \mathbb{D}^{\Omega}_{\boldsymbol{\rho\rho\rho}} = \int_{\Omega} \frac{(\boldsymbol{\rho}\cdot\boldsymbol{\kappa}_z)\boldsymbol{\rho}\otimes\boldsymbol{\rho}\otimes\boldsymbol{\rho}}{\boldsymbol{\rho}\cdot\boldsymbol{\rho}}dA \tag{18}$$

In order to transform the previous domain integrals into boundary integrals we apply Gauss theorem in the generalized form illustrated in D'Urso (2013a, 2014a). In this way the singularity at $\boldsymbol{\rho} = \boldsymbol{o}$ of the four domain integrals can be correctly taken into account.

2.1 Analytical expression of the gravity anomaly at O in terms of boundary integral

Let us now illustrate a general approach to express the 2D integrals in (16) as 1D integrals extended to the boundary of Ω. Generality lies in the fact that, owing to the symmetry of the integrals, application of Gauss theorem can be based upon a unique formula. Actually, we are going to prove the general formula

$$\int_{\Omega} \frac{\iota_{\boldsymbol{\rho}}[\otimes\boldsymbol{\rho},m]}{\boldsymbol{\rho}\cdot\boldsymbol{\rho}}dA = \frac{1}{m+1}\int_{\partial\Omega} \frac{\iota_{\boldsymbol{\rho}}[\otimes\boldsymbol{\rho},m](\boldsymbol{\rho}\cdot\boldsymbol{\nu})}{\boldsymbol{\rho}\cdot\boldsymbol{\rho}}ds \quad m=0,1,\ldots \tag{19}$$

where $\iota_{\boldsymbol{\rho}} = \boldsymbol{\rho}\cdot\boldsymbol{\kappa}_z$, $\boldsymbol{\nu}$ is the 2D outward unit normal to $\partial\Omega$ and $[\otimes\boldsymbol{\rho},m]$ denotes a rank-m tensor defined by

$$[\otimes\boldsymbol{\rho},m] = \begin{cases} 1 & \text{if} \quad m=0 \\ \boldsymbol{\rho} & \text{if} \quad m=1 \\ \boldsymbol{\rho}\otimes\boldsymbol{\rho} & \text{if} \quad m=2 \\ \cdots\cdots\cdots & \cdots\cdots\cdots\cdots \\ \underbrace{\boldsymbol{\rho}\otimes\boldsymbol{\rho}\otimes\cdots\otimes\boldsymbol{\rho}}_{m\ times} & \text{if} \quad m>2 \end{cases} \tag{20}$$

To fix the ideas we shall prove the identity (19) for $m = 2$

$$\int_{\Omega} \frac{\iota_{\rho}\boldsymbol{\rho}\otimes\boldsymbol{\rho}}{\boldsymbol{\rho}\cdot\boldsymbol{\rho}} dA = \frac{1}{3}\int_{\partial\Omega} \frac{\iota_{\rho}(\boldsymbol{\rho}\otimes\boldsymbol{\rho})\nu_{\rho}}{\boldsymbol{\rho}\cdot\boldsymbol{\rho}} ds \tag{21}$$

since it allows us to illustrate our approach to a degree of generality sufficient to extend the final result to all integrals in (16) and to the additional ones, not reported in (16), containing tensors of rank superior to three, i.e. tensors of the kind $[\otimes\boldsymbol{\rho}, m]$ where $m > 3$. In the following we shall make use of some differential identities which are collected in Appendix A in order to not divert the reader from the main stream of our derivation.

Let us consider the following identity involving the divergence of a rank-three tensor.

$$\begin{aligned}\operatorname{div}\Big[\iota_{\rho}(\boldsymbol{\rho}\otimes\boldsymbol{\rho})\otimes\frac{\boldsymbol{\rho}}{\boldsymbol{\rho}\cdot\boldsymbol{\rho}}\Big] &= \Big[(\boldsymbol{\rho}\otimes\boldsymbol{\rho})\otimes\frac{\boldsymbol{\rho}}{\boldsymbol{\rho}\cdot\boldsymbol{\rho}}\Big]\operatorname{grad}\iota_{\rho} + \iota_{\rho}\Big[(\operatorname{grad}\boldsymbol{\rho})\frac{\boldsymbol{\rho}}{\boldsymbol{\rho}\cdot\boldsymbol{\rho}}\Big]\otimes\boldsymbol{\rho} + \\ &+ \iota_{\rho}\boldsymbol{\rho}\otimes\Big[(\operatorname{grad}\boldsymbol{\rho})\frac{\boldsymbol{\rho}}{\boldsymbol{\rho}\cdot\boldsymbol{\rho}}\Big] + \iota_{\rho}(\boldsymbol{\rho}\otimes\boldsymbol{\rho})\operatorname{div}\frac{\boldsymbol{\rho}}{\boldsymbol{\rho}\cdot\boldsymbol{\rho}}\end{aligned} \tag{22}$$

which stems from the identity (119) of Appendix A. Furthermore, application of the identity (120) provides

$$\operatorname{grad}\iota_{\rho} = \operatorname{grad}(\boldsymbol{\rho}\cdot\boldsymbol{\kappa}_z) = (\operatorname{grad}\boldsymbol{\rho})^t\boldsymbol{\kappa}_z = \boldsymbol{\kappa}_z \tag{23}$$

since $\boldsymbol{\kappa}_z$ is a constant vector field and $\operatorname{grad}\boldsymbol{\rho} = \mathbf{I}$ where $\mathbf{I}$ is the rank-two identity tensor. Substituting the previous relation in (22) one obtains

$$\begin{aligned}\operatorname{div}\Big[\iota_{\rho}(\boldsymbol{\rho}\otimes\boldsymbol{\rho})\otimes\frac{\boldsymbol{\rho}}{\boldsymbol{\rho}\cdot\boldsymbol{\rho}}\Big] &= \Big[(\boldsymbol{\rho}\otimes\boldsymbol{\rho})\otimes\frac{\boldsymbol{\rho}}{\boldsymbol{\rho}\cdot\boldsymbol{\rho}}\Big]\boldsymbol{\kappa}_z + \iota_{\rho}\Big[\frac{\boldsymbol{\rho}}{\boldsymbol{\rho}\cdot\boldsymbol{\rho}}\otimes\boldsymbol{\rho} + \boldsymbol{\rho}\otimes\frac{\boldsymbol{\rho}}{\boldsymbol{\rho}\cdot\boldsymbol{\rho}}\Big] + \\ &+ \iota_{\rho}(\boldsymbol{\rho}\otimes\boldsymbol{\rho})\operatorname{div}\frac{\boldsymbol{\rho}}{\boldsymbol{\rho}\cdot\boldsymbol{\rho}} = \\ &= 3\iota_{\rho}\frac{\boldsymbol{\rho}\otimes\boldsymbol{\rho}}{\boldsymbol{\rho}\cdot\boldsymbol{\rho}} + \iota_{\rho}(\boldsymbol{\rho}\otimes\boldsymbol{\rho})\operatorname{div}\frac{\boldsymbol{\rho}}{\boldsymbol{\rho}\cdot\boldsymbol{\rho}}\end{aligned} \tag{24}$$

Finally, integrating the previous identity over Ω yields

$$\int_{\Omega}\iota_{\rho}\frac{\boldsymbol{\rho}\otimes\boldsymbol{\rho}}{\boldsymbol{\rho}\cdot\boldsymbol{\rho}}dA = \frac{1}{3}\int_{\Omega}\operatorname{div}\Big[\iota_{\rho}(\boldsymbol{\rho}\otimes\boldsymbol{\rho})\otimes\frac{\boldsymbol{\rho}}{\boldsymbol{\rho}\cdot\boldsymbol{\rho}}\Big]dA - \frac{1}{3}\int_{\Omega}\iota_{\rho}(\boldsymbol{\rho}\otimes\boldsymbol{\rho})\operatorname{div}\frac{\boldsymbol{\rho}}{\boldsymbol{\rho}\cdot\boldsymbol{\rho}}dA \tag{25}$$

The second integral on the right-hand side can be computed by means of the general result (Tang, 2006)

$$\int_{F}\varphi(\boldsymbol{\rho})\operatorname{div}\Big[\frac{\boldsymbol{\rho}}{\boldsymbol{\rho}\cdot\boldsymbol{\rho}}\Big]dA = \begin{cases} 0 & \text{if} \quad \boldsymbol{o}\notin F \\ \alpha(\boldsymbol{o})\varphi(\boldsymbol{o}) & \text{if} \quad \boldsymbol{o}\in F\end{cases} \tag{26}$$

where φ is a scalar function and F denotes an arbitrary 2D domain. The previous expression can be extended to arbitrary tensors by applying it to each scalar component of the tensor. Furthermore, the quantity α represents the angular measure, expressed in radians, of the intersection between F and a circular neighbourhood of the singularity point $\boldsymbol{\rho} = \boldsymbol{o}$, see D'Urso (2012, 2013a, 2014a) for additional details. Although its computation is not required in the ensuing developments, we specify for completeness that α can be computed by means of the general algorithm detailed in D'Urso and Russo (2002).

On account of (26) one infers that the second integral on the right-hand side of (25) is the null rank-two tensor **O** since

$$\int_{\Omega} \iota_{\rho}(\boldsymbol{\rho}\otimes\boldsymbol{\rho})\,\mathrm{div}\,\frac{\boldsymbol{\rho}}{\boldsymbol{\rho}\cdot\boldsymbol{\rho}}dA = \begin{cases} \mathbf{O} & \text{if} \quad \boldsymbol{o}\notin\Omega \\ [\iota_{\rho}\boldsymbol{\rho}\otimes\boldsymbol{\rho}]_{\boldsymbol{\rho}=\boldsymbol{o}}\,\alpha(\boldsymbol{o}) & \text{if} \quad \boldsymbol{o}\in\Omega \end{cases} \tag{27}$$

However, the expression $[\iota_{\rho}(\boldsymbol{\rho}\otimes\boldsymbol{\rho})]_{\boldsymbol{\rho}=\boldsymbol{o}}$ amounts to evaluating the quantity $\iota_{\rho}(\boldsymbol{\rho}\otimes\boldsymbol{\rho})$ at the singularity point $\boldsymbol{\rho}=\boldsymbol{o}$, what yields trivially the null tensor **O**. Hence, according to (27), the last integral in (25) is always the null tensor, independently from the position of singularity point $\boldsymbol{\rho}=\boldsymbol{o}$ with respect to the domain Ω of integration. In conclusion, upon application of Gauss theorem to the second integral in (25), we finally infer the identity (21). Remarkably, the derivation of this identity has also allowed us to prove that the singularity at $\boldsymbol{\rho}=\boldsymbol{o}$, of the integrand function appearing on the left-hand side of (21), can be actually ignored.

Furthermore, it is not difficult to rephrase the path of reasoning detailed in formulas (22)-(27) so as to prove the more general formula (19). Hence, defining

$$d_{\rho}^{\partial\Omega} = \int_{\partial\Omega} \frac{(\boldsymbol{\rho}\cdot\boldsymbol{\kappa}_z)(\boldsymbol{\rho}\cdot\boldsymbol{\nu})}{\boldsymbol{\rho}\cdot\boldsymbol{\rho}}ds \qquad \mathbf{d}_{\rho}^{\partial\Omega} = \int_{\partial\Omega} \frac{(\boldsymbol{\rho}\cdot\boldsymbol{\kappa}_z)\boldsymbol{\rho}(\boldsymbol{\rho}\cdot\boldsymbol{\nu})}{\boldsymbol{\rho}\cdot\boldsymbol{\rho}}ds \tag{28}$$

$$\mathbf{D}_{\rho\rho}^{\partial\Omega} = \int_{\partial\Omega} \frac{(\boldsymbol{\rho}\cdot\boldsymbol{\kappa}_z)\boldsymbol{\rho}\otimes\boldsymbol{\rho}(\boldsymbol{\rho}\cdot\boldsymbol{\nu})}{\boldsymbol{\rho}\cdot\boldsymbol{\rho}}ds \qquad \mathbb{D}_{\rho\rho\rho}^{\partial\Omega} = \int_{\partial\Omega} \frac{(\boldsymbol{\rho}\cdot\boldsymbol{\kappa}_z)\boldsymbol{\rho}\otimes\boldsymbol{\rho}\otimes\boldsymbol{\rho}(\boldsymbol{\rho}\cdot\boldsymbol{\nu})}{\boldsymbol{\rho}\cdot\boldsymbol{\rho}}ds \tag{29}$$

one has, recalling definitions (17)-(18)

$$d_{\rho}^{\Omega} = d_{\rho}^{\partial\Omega} \qquad \mathbf{d}_{\rho}^{\Omega} = \frac{\mathbf{d}_{\rho}^{\partial\Omega}}{2} \qquad \mathbf{D}_{\rho\rho}^{\Omega} = \frac{\mathbf{D}_{\rho\rho}^{\partial\Omega}}{3} \qquad \mathbb{D}_{\rho\rho\rho}^{\Omega} = \frac{\mathbb{D}_{\rho\rho\rho}^{\partial\Omega}}{4} \tag{30}$$

In conclusion, application of formula (19) to (16) yields

$$\mathbf{g}_z(\boldsymbol{o}) = 2G\Big[\theta_{\boldsymbol{o}} d_{\rho}^{\partial\Omega} + \frac{\mathbf{c}\cdot\mathbf{d}_{\rho}^{\partial\Omega}}{2} + \frac{\mathbf{C}\cdot\mathbf{D}_{\rho\rho}^{\partial\Omega}}{3} + \frac{\mathbb{C}\cdot\mathbb{D}_{\rho\rho\rho}^{\partial\Omega}}{4}\Big] \tag{31}$$

a formula that will be specialized to the case of polygonal domains in the next subsection.

2.2 Algebraic expression of the gravity anomaly at O

In order to derive an algebraic expression suitable to be programmed we specialize formula (31) to the case of a polygonal domain Ω. Actually, this is by far the most common case since geological formations are either polygonal or can be approximated to polygons by subdividing the real boundary by an arbitrary number of vertices and edges. Once again, in order to illustrate the rationale of our derivation, we shall make reference to formula (21). In particular, denoting by n the common number of vertices and edges belonging to $\partial\Omega$ (see Fig. 1), formula (21) specializes to

$$\int_{\Omega} \frac{\iota_{\rho}\boldsymbol{\rho}\otimes\boldsymbol{\rho}}{\boldsymbol{\rho}\cdot\boldsymbol{\rho}}dA = \frac{1}{3}\sum_{i=1}^{n}\int_{\partial_i\Omega} \frac{[\boldsymbol{\rho}(s_i)\cdot\boldsymbol{\kappa}_z][\boldsymbol{\rho}(s_i)\otimes\boldsymbol{\rho}(s_i)][\boldsymbol{\rho}(s_i)\cdot\boldsymbol{\nu}(s_i)]}{\boldsymbol{\rho}(s_i)\cdot\boldsymbol{\rho}(s_i)}ds_i \tag{32}$$

where s_i is the curvilinear abscissa along the i-th edge $\partial_i\Omega$ of the boundary of Ω.

The edge $\partial_i\Omega$ connects the vertices $\boldsymbol{\rho}_i$ and $\boldsymbol{\rho}_{i+1}$, see, e.g., fig. 1, and it will be assumed that, along each edge, the relevant curvilinear abscissa has its origin at the i-th vertex. Being the product $\boldsymbol{\rho}(s_i)\cdot\boldsymbol{\nu}(s_i)$ constant along each side, formula (32) becomes

$$\int_{\Omega} \frac{\iota_{\rho}\mathbf{D}_{\rho\rho}}{\boldsymbol{\rho}\cdot\boldsymbol{\rho}} dA = \frac{1}{3}\sum_{i=1}^{n}\boldsymbol{\rho}_i\cdot\boldsymbol{\nu}_i \int_{\partial_i\Omega} \frac{[\boldsymbol{\rho}(s_i)\cdot\boldsymbol{\kappa}_z][\boldsymbol{\rho}(s_i)\otimes\boldsymbol{\rho}(s_i)]}{\boldsymbol{\rho}(s_i)\cdot\boldsymbol{\rho}(s_i)} ds_i \tag{33}$$

where $\boldsymbol{\nu}_i$ is the outward unit normal to the i-th edge. Assuming a counter-clockwise circulation sense along $\partial_i\Omega$ and denoting by $l_i = |\boldsymbol{\rho}_{i+1} - \boldsymbol{\rho}_i|$ the length of the i-th edge, it turns out $\boldsymbol{\nu}_i = (\boldsymbol{\rho}_{i+1} - \boldsymbol{\rho}_i)^{\perp}/l_i$ where $(\cdot)^{\perp}$ denotes a clockwise rotation of $(\cdot)$. In particular, $\boldsymbol{\rho}_i\cdot\boldsymbol{\nu}_i = \boldsymbol{\rho}_i\cdot\boldsymbol{\rho}_{i+1}^{\perp}/l_i$ where $\boldsymbol{\rho}_{i+1}^{\perp} = (z_{i+1}, -x_{i+1})$, (D'Urso, 2013a).

Introducing in (32) the adimensional abscissa $\lambda_i = s_i/l_i$ we finally get

$$\int_{\Omega} \frac{\iota_{\rho}\mathbf{D}_{\rho\rho}}{\boldsymbol{\rho}\cdot\boldsymbol{\rho}} dA = \frac{1}{3}\sum_{i=1}^{n}\boldsymbol{\rho}_i\cdot\boldsymbol{\rho}_{i+1}^{\perp} \int_{0}^{1} \frac{[\boldsymbol{\rho}(\lambda_i)\cdot\boldsymbol{\kappa}_z][\boldsymbol{\rho}(\lambda_i)\otimes\boldsymbol{\rho}(\lambda_i)]}{\boldsymbol{\rho}(\lambda_i)\cdot\boldsymbol{\rho}(\lambda_i)} d\lambda_i \tag{34}$$

which represents the starting point to derive the basic formulas useful for programming.

Actually, defining

$$d_{\boldsymbol{\rho}}^{\partial_i\Omega} = \int_{0}^{1} \frac{\boldsymbol{\rho}(\lambda_i)\cdot\boldsymbol{\kappa}_z}{\boldsymbol{\rho}(\lambda_i)\cdot\boldsymbol{\rho}(\lambda_i)} d\lambda_i \qquad \mathbf{d}_{\boldsymbol{\rho}}^{\partial_i\Omega} = \int_{0}^{1} \frac{[\boldsymbol{\rho}(\lambda_i)\cdot\boldsymbol{\kappa}_z]\boldsymbol{\rho}(\lambda_i)}{\boldsymbol{\rho}(\lambda_i)\cdot\boldsymbol{\rho}(\lambda_i)} d\lambda_i \tag{35}$$

$$\mathbf{D}_{\rho\rho}^{\partial_i\Omega} = \int_{0}^{1} \frac{[\boldsymbol{\rho}(\lambda_i)\cdot\boldsymbol{\kappa}_z]\boldsymbol{\rho}(\lambda_i)\otimes\boldsymbol{\rho}(\lambda_i)}{\boldsymbol{\rho}(\lambda_i)\cdot\boldsymbol{\rho}(\lambda_i)} d\lambda_i \tag{36}$$

$$\mathbb{D}_{\rho\rho\rho}^{\partial_i\Omega} = \int_{0}^{1} \frac{[\boldsymbol{\rho}(\lambda_i)\cdot\boldsymbol{\kappa}_z]\boldsymbol{\rho}(\lambda_i)\otimes\boldsymbol{\rho}(\lambda_i)\otimes\boldsymbol{\rho}(\lambda_i)}{\boldsymbol{\rho}(\lambda_i)\cdot\boldsymbol{\rho}(\lambda_i)} d\lambda_i \tag{37}$$

we can express the integrals (28)-(29) as

$$d_{\boldsymbol{\rho}}^{\partial\Omega} = \sum_{i=1}^{n}(\boldsymbol{\rho}_i\cdot\boldsymbol{\nu}_i)l_i d_{\boldsymbol{\rho}}^{\partial_i\Omega} \qquad \mathbf{d}_{\boldsymbol{\rho}}^{\partial\Omega} = \sum_{i=1}^{n}(\boldsymbol{\rho}_i\cdot\boldsymbol{\nu}_i)l_i \mathbf{d}_{\boldsymbol{\rho}}^{\partial_i\Omega} \tag{38}$$

$$\mathbf{D}_{\rho\rho}^{\partial\Omega} = \sum_{i=1}^{n}(\boldsymbol{\rho}_i\cdot\boldsymbol{\nu}_i)l_i \mathbf{D}_{\rho\rho}^{\partial_i\Omega} \qquad \mathbb{D}_{\rho\rho\rho}^{\partial\Omega} = \sum_{i=1}^{n}(\boldsymbol{\rho}_i\cdot\boldsymbol{\nu}_i)l_i \mathbb{D}_{\rho\rho\rho}^{\partial_i\Omega} \tag{39}$$

Accordingly, formula (31) of the gravity anomaly specializes as follows

$$\mathbf{g}_z(\boldsymbol{o}) = 2G\sum_{i=1}^{n}(\boldsymbol{\rho}_i\cdot\boldsymbol{\rho}_{i+1}^{\perp})\Big\{\theta_{\boldsymbol{o}} d_{\boldsymbol{\rho}}^{\partial_i\Omega} + \frac{\mathbf{c}\cdot\mathbf{d}_{\boldsymbol{\rho}}^{\partial_i\Omega}}{2} + \frac{\mathbf{C}\cdot\mathbf{D}_{\rho\rho}^{\partial_i\Omega}}{3} + \frac{\mathbb{C}\cdot\mathbb{D}_{\rho\rho\rho}^{\partial_i\Omega}}{4}\Big\} \tag{40}$$

The previous integrals can be evaluated analytically by introducing the following parameterization of the i-th edge

$$\boldsymbol{\rho}(\lambda_i) = \boldsymbol{\rho}_i + \lambda_i(\boldsymbol{\rho}_{i+1} - \boldsymbol{\rho}_i) = \boldsymbol{\rho}_i + \lambda_i\Delta\boldsymbol{\rho}_i \tag{41}$$

In this way one has

$$\boldsymbol{\rho}(\lambda_i)\cdot\boldsymbol{\kappa}_z = (\boldsymbol{\rho}_i\cdot\boldsymbol{\kappa}_z)+\lambda_i(\Delta\boldsymbol{\rho}_i\cdot\boldsymbol{\kappa}_z) = a_i + b_i\lambda_i \tag{42}$$

and

$$\boldsymbol{\rho}(\lambda_i)\cdot\boldsymbol{\rho}(\lambda_i) = p_i\lambda_i^2 + 2q_i\lambda_i + u_i \tag{43}$$

where

$$p_i = \Delta\boldsymbol{\rho}_i\cdot\Delta\boldsymbol{\rho}_i \qquad q_i = \boldsymbol{\rho}_i\cdot\Delta\boldsymbol{\rho}_i \qquad u_i = \boldsymbol{\rho}_i\cdot\boldsymbol{\rho}_i \tag{44}$$

Furthermore

$$\begin{aligned}\boldsymbol{\rho}(\lambda_i)\otimes\boldsymbol{\rho}(\lambda_i) &= \boldsymbol{\rho}_i\otimes\boldsymbol{\rho}_i + \lambda_i(\boldsymbol{\rho}_i\otimes\Delta\boldsymbol{\rho}_i + \Delta\boldsymbol{\rho}_i\otimes\boldsymbol{\rho}_i) + \lambda_i^2\Delta\boldsymbol{\rho}_i\otimes\Delta\boldsymbol{\rho}_i = \\ &= \mathbf{D}_{\boldsymbol{\rho}_i\boldsymbol{\rho}_i} + \lambda_i\mathbf{D}_{\boldsymbol{\rho}_i\Delta\boldsymbol{\rho}_i} + \lambda_i^2\mathbf{D}_{\Delta\boldsymbol{\rho}_i\Delta\boldsymbol{\rho}_i}\end{aligned} \tag{45}$$

Analogously, setting

$$\mathbb{D}_{\boldsymbol{\rho}_i\boldsymbol{\rho}_i\boldsymbol{\rho}_i} = \boldsymbol{\rho}_i\otimes\boldsymbol{\rho}_i\otimes\boldsymbol{\rho}_i \qquad \mathbb{D}_{\boldsymbol{\rho}_i\boldsymbol{\rho}_i\Delta\boldsymbol{\rho}_i} = \boldsymbol{\rho}_i\otimes\boldsymbol{\rho}_i\otimes\Delta\boldsymbol{\rho}_i + \boldsymbol{\rho}_i\otimes\Delta\boldsymbol{\rho}_i\otimes\boldsymbol{\rho}_i + \Delta\boldsymbol{\rho}_i\otimes\boldsymbol{\rho}_i\otimes\boldsymbol{\rho}_i \tag{46}$$

$$\mathbb{D}_{\boldsymbol{\rho}_i\Delta\boldsymbol{\rho}_i\Delta\boldsymbol{\rho}_i} = \boldsymbol{\rho}_i\otimes\Delta\boldsymbol{\rho}_i\otimes\Delta\boldsymbol{\rho}_i + \Delta\boldsymbol{\rho}_i\otimes\boldsymbol{\rho}_i\otimes\Delta\boldsymbol{\rho}_i + \Delta\boldsymbol{\rho}_i\otimes\Delta\boldsymbol{\rho}_i\otimes\boldsymbol{\rho}_i \tag{47}$$

$$\mathbb{D}_{\Delta\boldsymbol{\rho}_i\Delta\boldsymbol{\rho}_i\Delta\boldsymbol{\rho}_i} = \Delta\boldsymbol{\rho}_i\otimes\Delta\boldsymbol{\rho}_i\otimes\Delta\boldsymbol{\rho}_i \tag{48}$$

one has

$$\boldsymbol{\rho}(\lambda_i)\otimes\boldsymbol{\rho}(\lambda_i)\otimes\boldsymbol{\rho}(\lambda_i) = \mathbb{D}_{\boldsymbol{\rho}_i\boldsymbol{\rho}_i\boldsymbol{\rho}_i} + \lambda_i\mathbb{D}_{\boldsymbol{\rho}_i\boldsymbol{\rho}_i\Delta\boldsymbol{\rho}_i} + \lambda_i^2\mathbb{D}_{\boldsymbol{\rho}_i\Delta\boldsymbol{\rho}_i\Delta\boldsymbol{\rho}_i} + \lambda_i^3\mathbb{D}_{\Delta\boldsymbol{\rho}_i\Delta\boldsymbol{\rho}_i\Delta\boldsymbol{\rho}_i} \tag{49}$$

Thus, defining

$$f(\lambda_i) = \frac{a_i + b_i\lambda_i}{p_i\lambda_i^2 + 2q_i\lambda_i + u_i} \tag{50}$$

formula (40) specializes to

$$\begin{aligned}\mathbf{g}_z(\boldsymbol{o}) &= 2G\sum_{i=1}^{n}(\boldsymbol{\rho}_i\cdot\boldsymbol{\rho}_{i+1}^{\perp})\Big\{\theta_{\boldsymbol{o}}\int_0^1 f(\lambda_i)d\lambda_i + \frac{\mathbf{c}}{2}\cdot\int_0^1 f(\lambda_i)(\boldsymbol{\rho}_i + \lambda_i\Delta\boldsymbol{\rho}_i)d\lambda_i + \\ &+\frac{\mathbf{C}}{3}\cdot\int_0^1 f(\lambda_i)\Big[\mathbf{D}_{\boldsymbol{\rho}_i\boldsymbol{\rho}_i} + \lambda_i\mathbf{D}_{\boldsymbol{\rho}_i\Delta\boldsymbol{\rho}_i} + \lambda_i^2\mathbf{D}_{\Delta\boldsymbol{\rho}_i\Delta\boldsymbol{\rho}_i}\Big]d\lambda_i + \\ &+\frac{\mathbb{C}}{4}\cdot\int_0^1 f(\lambda_i)\Big[\mathbb{C}_{\boldsymbol{\rho}_i\boldsymbol{\rho}_i\boldsymbol{\rho}_i} + \lambda_i\mathbb{C}_{\boldsymbol{\rho}_i\boldsymbol{\rho}_i\Delta\boldsymbol{\rho}_i} + \lambda_i^2\mathbb{C}_{\boldsymbol{\rho}_i\Delta\boldsymbol{\rho}_i\Delta\boldsymbol{\rho}_i} + \lambda_i^3\mathbb{C}_{\Delta\boldsymbol{\rho}_i\Delta\boldsymbol{\rho}_i\Delta\boldsymbol{\rho}_i}\Big]d\lambda_i\Big\}\end{aligned} \tag{51}$$

Grouping together the quantities multiplying the same exponent of λ_i and setting

$$\theta^O_{\boldsymbol{\rho}_i} = \frac{\mathbf{c}\cdot\boldsymbol{\rho}_i}{2} + \frac{\mathbf{C}\cdot\mathbf{D}_{\boldsymbol{\rho}_i\boldsymbol{\rho}_i}}{3} + \frac{\mathbb{C}\cdot\mathbb{D}_{\boldsymbol{\rho}_i\boldsymbol{\rho}_i\boldsymbol{\rho}_i}}{4} \tag{52}$$

$$\theta^O_{\Delta\boldsymbol{\rho}_i} = \frac{\mathbf{c}\cdot\Delta\boldsymbol{\rho}_i}{2} + \frac{\mathbf{C}\cdot\mathbf{D}_{\boldsymbol{\rho}_i\Delta\boldsymbol{\rho}_i}}{3} + \frac{\mathbb{C}\cdot\mathbb{D}_{\boldsymbol{\rho}_i\boldsymbol{\rho}_i\Delta\boldsymbol{\rho}_i}}{4} \tag{53}$$

$$\theta^O_{\Delta\rho_i\Delta\rho_i} = \frac{\mathbf{C}\cdot\mathbf{D}_{\Delta\rho_i\Delta\rho_i}}{3} + \frac{\mathbb{C}\cdot\mathbb{D}_{\rho_i\Delta\rho_i\Delta\rho_i}}{4} \tag{54}$$

$$\theta^O_{\Delta\rho_i\Delta\rho_i\Delta\rho_i} = \frac{\mathbb{C}\cdot\mathbb{D}_{\Delta\rho_i\Delta\rho_i\Delta\rho_i}}{4} \tag{55}$$

formula (40) becomes

$$\begin{aligned}\mathbf{g}_z(\boldsymbol{o}) = 2G\sum_{i=1}^{n}(\boldsymbol{\rho}_i\cdot\boldsymbol{\rho}^{\perp}_{i+1})\Big\{&I_{0i}\Big[a_i(\theta_{\boldsymbol{o}}+\theta^O_{\boldsymbol{\rho}_i})\Big]+I_{1i}\Big[a_i\theta^O_{\Delta\boldsymbol{\rho}_i}+b_i\theta^O_{\boldsymbol{\rho}_i}\Big]+\\ &+I_{2i}\Big[a_i\theta^O_{\Delta\boldsymbol{\rho}_i\Delta\boldsymbol{\rho}_i}+b_i\theta^O_{\Delta\boldsymbol{\rho}_i}\Big]+I_{3i}\Big[a_i\theta^O_{\Delta\boldsymbol{\rho}_i\Delta\boldsymbol{\rho}_i\Delta\boldsymbol{\rho}_i}+b_i\theta^O_{\Delta\boldsymbol{\rho}_i\Delta\boldsymbol{\rho}_i}\Big]+I_{4i}b_i\theta^O_{\Delta\boldsymbol{\rho}_i\Delta\boldsymbol{\rho}_i\Delta\boldsymbol{\rho}_i}\Big\}\end{aligned} \tag{56}$$

where

$$I_{ki} = \int_0^1 \frac{\lambda_i^k}{p_i\lambda_i^2+2q_i\lambda_i+u_i}d\lambda_i \tag{57}$$

$\theta_{\boldsymbol{o}}$ is defined in (13), a_i, b_i in (42), $\theta^O_{\boldsymbol{\rho}_i}$-$\theta^O_{\Delta\boldsymbol{\rho}_i}$-$\theta^O_{\Delta\boldsymbol{\rho}_i\Delta\boldsymbol{\rho}_i}$- $\theta^O_{\Delta\boldsymbol{\rho}_i\Delta\boldsymbol{\rho}_i\Delta\boldsymbol{\rho}_i}$ in (52)-(55).

The actual computation of the integrals I_{ki} will be detailed in section 4. In particular, singuarities in their expression, due to the vanishing of the denominator in (57), will be proved to be ineffective. Hence, formula (56) is singularity-free in the sense that, for edges characterized by singularities of the integrals I_{ki}, the whole addend of the sum is zero.

3 Gravity anomaly of a 2D body at an arbitrary point P

Gravity anomaly calculations at an observation point which does not coincide with the origin of the reference frame have been first addressed by Zhou (2010). Specifically, the author devised two alternative formulations: the first one, named Coordinate Transformation, was conceived so as to make the observation point as the origin of the new coordinate system and employing the solution obtained by the author in Zhang et al (2001) and Zhou (2009a). Clearly, this approach requires to express the density contrast as function of the new coordinates. In the second formulation proposed by Zhou (2010), named Solution Transformation, the solution at an arbitrary point is extrapolated from that obtained at the origin of the reference frame.

On the contrary, denoting by $\boldsymbol{\omega} = (x_P, z_P)$ the position vector of an arbitrary point P, we show that the approach illustrated in the previous section, as well as the function expressing the density contrast, can be left unchanged provided that one introduces the vector

$$\boldsymbol{\rho} = \boldsymbol{\sigma} - \boldsymbol{\omega} \tag{58}$$

defining the relative position of the generic point $\boldsymbol{\sigma} = (x, z)$ of Ω with respect to P, see, e.g., fig. 2. Hence the gravity anomaly at P is given by

$$\mathbf{g}_z(P) = \mathbf{g}_z(\omega) = 2G\int_{\Omega}\frac{\theta(\boldsymbol{\sigma})(\boldsymbol{\rho}\cdot\boldsymbol{\kappa}_z)}{\boldsymbol{\rho}\cdot\boldsymbol{\rho}}dA \tag{59}$$

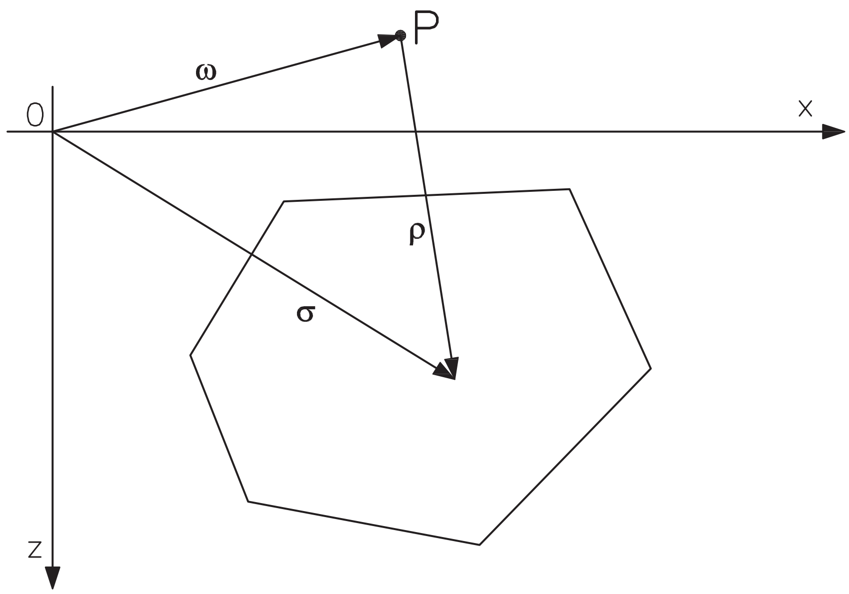

Fig. 2 Representation of geometric quantities used to assign density contrast ($\boldsymbol{\sigma}$) and define the position of Ω with respect to an arbitray point P

an expression which trivially specializes to (6) whenever $\boldsymbol{\omega} = \boldsymbol{o}$. On account of (7) the previous expression becomes

$$\mathbf{g}_z(\boldsymbol{\omega}) = 2G\Big\{\theta_{\boldsymbol{o}} \int_{\Omega} \frac{\iota_\rho}{\boldsymbol{\rho}\cdot\boldsymbol{\rho}} dA + \mathbf{c}\cdot \int_{\Omega} \frac{\iota_\rho \boldsymbol{\sigma}}{\boldsymbol{\rho}\cdot\boldsymbol{\rho}} dA + \mathbf{C}\cdot \int_{\Omega} \frac{\iota_\rho \mathbf{D}_{\sigma\sigma}}{\boldsymbol{\rho}\cdot\boldsymbol{\rho}} dA + \mathbb{C}\cdot \int_{\Omega} \frac{\iota_\rho \mathbb{D}_{\sigma\sigma\sigma}}{\boldsymbol{\rho}\cdot\boldsymbol{\rho}} dA\Big\} \tag{60}$$

where $\mathbf{D}_{\sigma\sigma}$ and $\mathbb{D}_{\sigma\sigma\sigma}$ are defined as in (8).

To exploit the results illustrated in the previous section, it is convenient to express $\boldsymbol{\sigma}$ as function of $\boldsymbol{\rho}$. For brevity this is detailed only for the rank-three tensor $\mathbb{D}_{\sigma\sigma\sigma}$ since it is the more cumbersome to handle. In particular, recalling (58), one has

$$\begin{aligned} \mathbb{D}_{\sigma\sigma\sigma} &= \boldsymbol{\sigma}\otimes\boldsymbol{\sigma}\otimes\boldsymbol{\sigma} = (\boldsymbol{\rho}+\boldsymbol{\omega})\otimes(\boldsymbol{\rho}+\boldsymbol{\omega})\otimes(\boldsymbol{\rho}+\boldsymbol{\omega}) = \\ &= \mathbb{D}_{\rho\rho\rho} + \mathbb{D}_{\rho\rho\omega} + \mathbb{D}_{\omega\omega\rho} + \mathbb{D}_{\omega\omega\omega} \end{aligned} \tag{61}$$

where $\mathbb{D}_{\omega\omega\omega} = \boldsymbol{\omega}\otimes\boldsymbol{\omega}\otimes\boldsymbol{\omega}$,

$$\mathbb{D}_{\rho\rho\omega} = \boldsymbol{\rho}\otimes\boldsymbol{\rho}\otimes\boldsymbol{\omega} + \boldsymbol{\rho}\otimes\boldsymbol{\omega}\otimes\boldsymbol{\rho} + \boldsymbol{\omega}\otimes\boldsymbol{\rho}\otimes\boldsymbol{\rho} \tag{62}$$

and

$$\begin{aligned} \mathbb{D}_{\omega\omega\rho} &= \boldsymbol{\omega}\otimes\boldsymbol{\omega}\otimes\boldsymbol{\rho} + \boldsymbol{\omega}\otimes\boldsymbol{\rho}\otimes\boldsymbol{\omega} + \boldsymbol{\rho}\otimes\boldsymbol{\omega}\otimes\boldsymbol{\omega} = \\ &= \mathbf{D}_{\omega\omega}\otimes\boldsymbol{\rho} + \boldsymbol{\omega}\otimes\boldsymbol{\rho}\otimes\boldsymbol{\omega} + \boldsymbol{\rho}\otimes\mathbf{D}_{\omega\omega} \end{aligned} \tag{63}$$

Hence, (60) becomes

$$\begin{aligned} \mathbf{g}_z(\boldsymbol{\omega}) &= 2G\Big\{[\theta_{\boldsymbol{o}} + \mathbf{c}\cdot\boldsymbol{\omega} + \mathbf{C}\cdot\mathbf{D}_{\omega\omega} + \mathbb{C}\cdot\mathbb{D}_{\omega\omega\omega}]d_\rho^{\Omega} + \mathbf{c}\cdot\mathbf{d}_\rho^{\Omega} + \\ &+\mathbf{C}\cdot[\mathbf{d}_\rho^{\Omega}\otimes\boldsymbol{\omega} + \boldsymbol{\omega}\otimes\mathbf{d}_\rho^{\Omega} + \mathbf{D}_{\rho\rho}^{\Omega}] + \mathbb{C}\cdot[\mathbf{D}_{\omega\omega}\otimes\mathbf{d}_\rho^{\Omega} + \boldsymbol{\omega}\otimes\mathbf{d}_\rho^{\Omega}\otimes\boldsymbol{\omega} + \mathbf{d}_\rho^{\Omega}\otimes\mathbf{D}_{\omega\omega}] + \\ &+\mathbb{C}\cdot[\mathbf{D}_{\rho\rho}^{\Omega}\otimes\boldsymbol{\omega} + \mathbf{d}_\rho^{\Omega}\otimes\boldsymbol{\omega}\otimes\mathbf{d}_\rho^{\Omega} + \boldsymbol{\omega}\otimes\mathbf{D}_{\rho\rho}^{\Omega}] + \mathbb{C}\cdot\mathbb{D}_{\rho\rho\rho}^{\Omega}\Big\} \end{aligned} \tag{64}$$

which represents the generalization of (16) to the case $\boldsymbol{\omega} \neq \boldsymbol{o}$.

Special attention has to be paid to the symbol $\mathbf{d}_{\boldsymbol{\rho}}^{\Omega} \otimes \boldsymbol{\omega} \otimes \mathbf{d}_{\boldsymbol{\rho}}^{\Omega}$ which is a shorthand to denote the third-order tensor

$$\mathbf{d}_{\boldsymbol{\rho}}^{\Omega} \otimes \boldsymbol{\omega} \otimes \mathbf{d}_{\boldsymbol{\rho}}^{\Omega} = \int_{\Omega} \frac{(\boldsymbol{\rho} \cdot \boldsymbol{\kappa}_z)\boldsymbol{\rho} \otimes \boldsymbol{\omega} \otimes \boldsymbol{\rho}}{\boldsymbol{\rho} \cdot \boldsymbol{\rho}} dA \tag{65}$$

In spite of its symbol, which has been adopted to emphasize its symmetric expression, the tensor above cannot be obtained as triple tensor product of the vectors $\mathbf{d}_{\boldsymbol{\rho}}^{\Omega}$ and $\boldsymbol{\omega}$. Rather, as detailed in subsection 3.3, it is conveniently computed starting from the rank-two tensor $\mathbf{D}_{\boldsymbol{\rho\rho}}^{\Omega}$. For sake of clarity, and to parallel the treatment developed in the previous section, we shall consider separately the analytical expression of the gravity attraction at an arbitrary point P and its algebraic counterpart, i.e. the formula useful for programming.

3.1 Analytical expression of the gravity anomaly at an arbitrary point P in terms of boundary integral

Although $\boldsymbol{\rho}$ is now defined from (58) it can be shown that formula (19) holds as well. Thus, recalling (30) and setting

$$\theta_{\omega} = \mathbf{c} \cdot \boldsymbol{\omega} + \mathbf{C} \cdot \mathbf{D}_{\omega\omega} + \mathbb{C} \cdot \mathbb{D}_{\omega\omega\omega} \tag{66}$$

formula (64) specializes to

$$\begin{aligned} \mathbf{g}_z(\boldsymbol{\omega}) = 2G\Big\{&(\theta_{\boldsymbol{o}} + \theta_{\omega}) d_{\boldsymbol{\rho}}^{\partial\Omega} + \frac{\mathbf{c} \cdot \mathbf{d}_{\boldsymbol{\rho}}^{\partial\Omega}}{2} + \mathbf{C} \cdot [\frac{\mathbf{d}_{\boldsymbol{\rho}}^{\partial\Omega}}{2} \otimes \boldsymbol{\omega} + \boldsymbol{\omega} \otimes \frac{\mathbf{d}_{\boldsymbol{\rho}}^{\partial\Omega}}{2} + \frac{\mathbf{D}_{\boldsymbol{\rho\rho}}^{\partial\Omega}}{3}] + \\ &+ \mathbb{C} \cdot \Big[\frac{1}{2}\Big(\mathbf{D}_{\omega\omega} \otimes \mathbf{d}_{\boldsymbol{\rho}}^{\partial\Omega} + \boldsymbol{\omega} \otimes \mathbf{d}_{\boldsymbol{\rho}}^{\partial\Omega} \otimes \boldsymbol{\omega} + \mathbf{d}_{\boldsymbol{\rho}}^{\partial\Omega} \otimes \mathbf{D}_{\omega\omega}\Big) + \\ &+ \frac{1}{3}\Big(\mathbf{D}_{\boldsymbol{\rho\rho}}^{\partial\Omega} \otimes \boldsymbol{\omega} + \mathbf{d}_{\boldsymbol{\rho}}^{\partial\Omega} \otimes \boldsymbol{\omega} \otimes \mathbf{d}_{\boldsymbol{\rho}}^{\partial\Omega} + \boldsymbol{\omega} \otimes \mathbf{D}_{\boldsymbol{\rho\rho}}^{\partial\Omega}\Big) + \frac{\mathbb{D}_{\boldsymbol{\rho\rho\rho}}^{\partial\Omega}}{4}\Big]\Big\} \end{aligned} \tag{67}$$

Obviously, (67) coincides with (31) when $\boldsymbol{\omega} = \boldsymbol{o}$. We are now in the position to specialize (67) to the case of a polygonal boundary.

3.2 Algebraic expression of the gravity anomaly at an arbitrary point P

On account of (38) and (39), formula (67) becomes

$$\begin{aligned} \mathbf{g}_z(\boldsymbol{\omega}) = 2G\sum_{i=1}^{n} \boldsymbol{\rho}_i \cdot \boldsymbol{\rho}_{i+1}^{\perp}\Big\{&[\theta_{\boldsymbol{o}} + \theta_{\omega}] d_{\boldsymbol{\rho}}^{\partial_i\Omega} + \frac{\mathbf{c} \cdot \mathbf{d}_{\boldsymbol{\rho}}^{\partial_i\Omega}}{2} + \mathbf{C} \cdot \Big[\frac{\mathbf{d}_{\boldsymbol{\rho}}^{\partial_i\Omega}}{2} \otimes \boldsymbol{\omega} + \boldsymbol{\omega} \otimes \frac{\mathbf{d}_{\boldsymbol{\rho}}^{\partial_i\Omega}}{2} + \frac{\mathbf{D}_{\boldsymbol{\rho\rho}}^{\partial_i\Omega}}{3}\Big] + \\ &+ \mathbb{C} \cdot \Big[\frac{1}{2}\Big(\mathbf{D}_{\omega\omega} \otimes \mathbf{d}_{\boldsymbol{\rho}}^{\partial_i\Omega} + \boldsymbol{\omega} \otimes \mathbf{d}_{\boldsymbol{\rho}}^{\partial_i\Omega} \otimes \boldsymbol{\omega} + \mathbf{d}_{\boldsymbol{\rho}}^{\partial_i\Omega} \otimes \mathbf{D}_{\omega\omega}\Big) + \frac{1}{3}\Big(\mathbf{D}_{\boldsymbol{\rho\rho}}^{\partial_i\Omega} \otimes \boldsymbol{\omega} + \\ &+ \mathbf{d}_{\boldsymbol{\rho}}^{\partial_i\Omega} \otimes \boldsymbol{\omega} \otimes \mathbf{d}_{\boldsymbol{\rho}}^{\partial_i\Omega} + \boldsymbol{\omega} \otimes \mathbf{D}_{\boldsymbol{\rho\rho}}^{\partial_i\Omega}\Big) + \frac{\mathbb{D}_{\boldsymbol{\rho\rho\rho}}^{\partial_i\Omega}}{4}\Big]\Big\} \end{aligned} \tag{68}$$

Furthermore, recalling the definitions (41)-(43), (45), (49) and (57) one can express (35)-(37)

$$d_{\boldsymbol{\rho}}^{\partial_i\Omega} = a_i I_{0i} + b_i I_{1i} \tag{69}$$

$$\mathbf{d}_{\boldsymbol{\rho}}^{\partial_i\Omega} = (a_i I_{0i} + b_i I_{1i})\boldsymbol{\rho}_i + (a_i I_{1i} + b_i I_{2i})\varDelta\boldsymbol{\rho}_i \tag{70}$$

$$\mathbf{D}_{\boldsymbol{\rho\rho}}^{\partial_i\Omega} = (a_i I_{0i} + b_i I_{1i})\mathbf{D}_{\boldsymbol{\rho}_i\boldsymbol{\rho}_i} + (a_i I_{1i} + b_i I_{2i})\mathbf{D}_{\boldsymbol{\rho}_i\varDelta\boldsymbol{\rho}_i} + (a_i I_{2i} + b_i I_{3i})\mathbf{D}_{\varDelta\boldsymbol{\rho}_i\varDelta\boldsymbol{\rho}_i} \tag{71}$$

$$\begin{aligned}\mathbb{D}_{\boldsymbol{\rho\rho\rho}}^{\partial_i\Omega} &= (a_i I_{0i} + b_i I_{1i})\mathbb{D}_{\boldsymbol{\rho}_i\boldsymbol{\rho}_i\boldsymbol{\rho}_i} + (a_i I_{1i} + b_i I_{2i})\mathbb{D}_{\boldsymbol{\rho}_i\boldsymbol{\rho}_i\varDelta\boldsymbol{\rho}_i} + \\ &+ (a_i I_{2i} + b_i I_{3i})\mathbb{D}_{\boldsymbol{\rho}_i\varDelta\boldsymbol{\rho}_i\varDelta\boldsymbol{\rho}_i} + (a_i I_{3i} + b_i I_{4i})\mathbb{D}_{\varDelta\boldsymbol{\rho}_i\varDelta\boldsymbol{\rho}_i\varDelta\boldsymbol{\rho}_i}\end{aligned} \tag{72}$$

In order to shorten the subsequent formulas to the maximum extent, it is convenient to introduce the following additional notation

$$\mathbf{D}_{\boldsymbol{\rho}_i\boldsymbol{\omega}} = \boldsymbol{\rho}_i \otimes \boldsymbol{\omega} + \boldsymbol{\omega} \otimes \boldsymbol{\rho}_i \qquad \mathbf{D}_{\varDelta\boldsymbol{\rho}_i\boldsymbol{\omega}} = \varDelta\boldsymbol{\rho}_i \otimes \boldsymbol{\omega} + \boldsymbol{\omega} \otimes \varDelta\boldsymbol{\rho}_i \tag{73}$$

and

$$\mathbb{D}_{\boldsymbol{\rho}_i\boldsymbol{\rho}_i\boldsymbol{\omega}} = \boldsymbol{\rho}_i \otimes \boldsymbol{\rho}_i \otimes \boldsymbol{\omega} + \cancel{\boldsymbol{\rho}_i \otimes \boldsymbol{\omega} \otimes \boldsymbol{\rho}_i} + \boldsymbol{\omega} \otimes \boldsymbol{\rho}_i \otimes \boldsymbol{\rho}_i = \mathbf{D}_{\boldsymbol{\rho}_i\boldsymbol{\rho}_i} \otimes \boldsymbol{\omega} + \boldsymbol{\omega} \otimes \mathbf{D}_{\boldsymbol{\rho}_i\boldsymbol{\rho}_i} \tag{74}$$

$$\begin{aligned}\mathbb{D}_{\boldsymbol{\rho}_i\varDelta\boldsymbol{\rho}_i\boldsymbol{\omega}} &= \boldsymbol{\rho}_i \otimes \varDelta\boldsymbol{\rho}_i \otimes \boldsymbol{\omega} + \varDelta\boldsymbol{\rho}_i \otimes \boldsymbol{\rho}_i \otimes \boldsymbol{\omega} + \boldsymbol{\omega} \otimes \boldsymbol{\rho}_i \otimes \varDelta\boldsymbol{\rho}_i + \boldsymbol{\omega} \otimes \varDelta\boldsymbol{\rho}_i \otimes \boldsymbol{\rho}_i + \\ &+ \cancel{\boldsymbol{\rho}_i \otimes \boldsymbol{\omega} \otimes \varDelta\boldsymbol{\rho}_i} + \cancel{\varDelta\boldsymbol{\rho}_i \otimes \boldsymbol{\omega} \otimes \boldsymbol{\rho}_i} = \\ &= \mathbf{D}_{\boldsymbol{\rho}_i\varDelta\boldsymbol{\rho}_i} \otimes \boldsymbol{\omega} + \boldsymbol{\omega} \otimes \mathbf{D}_{\boldsymbol{\rho}_i\varDelta\boldsymbol{\rho}_i}\end{aligned} \tag{75}$$

$$\begin{aligned}\mathbb{D}_{\varDelta\boldsymbol{\rho}_i\varDelta\boldsymbol{\rho}_i\boldsymbol{\omega}} &= \varDelta\boldsymbol{\rho}_i \otimes \varDelta\boldsymbol{\rho}_i \otimes \boldsymbol{\omega} + \boldsymbol{\omega} \otimes \varDelta\boldsymbol{\rho}_i \otimes \varDelta\boldsymbol{\rho}_i + \cancel{\varDelta\boldsymbol{\rho}_i \otimes \boldsymbol{\omega} \otimes \varDelta\boldsymbol{\rho}_i} = \\ &= \mathbf{D}_{\varDelta\boldsymbol{\rho}_i\varDelta\boldsymbol{\rho}_i} \otimes \boldsymbol{\omega} + \boldsymbol{\omega} \otimes \mathbf{D}_{\varDelta\boldsymbol{\rho}_i\varDelta\boldsymbol{\rho}_i}\end{aligned} \tag{76}$$

$$\begin{aligned}\mathbb{D}_{\boldsymbol{\omega\omega\rho}_i} &= \boldsymbol{\omega} \otimes \boldsymbol{\omega} \otimes \boldsymbol{\rho}_i + \boldsymbol{\omega} \otimes \boldsymbol{\rho}_i \otimes \boldsymbol{\omega} + \boldsymbol{\rho}_i \otimes \boldsymbol{\omega} \otimes \boldsymbol{\omega} = \\ &= \mathbf{D}_{\boldsymbol{\omega\omega}} \otimes \boldsymbol{\rho}_i + \boldsymbol{\omega} \otimes \boldsymbol{\rho}_i \otimes \boldsymbol{\omega} + \boldsymbol{\rho}_i \otimes \mathbf{D}_{\boldsymbol{\omega\omega}}\end{aligned} \tag{77}$$

$$\begin{aligned}\mathbb{D}_{\boldsymbol{\omega\omega}\varDelta\boldsymbol{\rho}_i} &= \boldsymbol{\omega} \otimes \boldsymbol{\omega} \otimes \varDelta\boldsymbol{\rho}_i + \boldsymbol{\omega} \otimes \varDelta\boldsymbol{\rho}_i \otimes \boldsymbol{\omega} + \varDelta\boldsymbol{\rho}_i \otimes \boldsymbol{\omega} \otimes \boldsymbol{\omega} = \\ &= \mathbf{D}_{\boldsymbol{\omega\omega}} \otimes \varDelta\boldsymbol{\rho}_i + \boldsymbol{\omega} \otimes \varDelta\boldsymbol{\rho}_i \otimes \boldsymbol{\omega} + \varDelta\boldsymbol{\rho}_i \otimes \mathbf{D}_{\boldsymbol{\omega\omega}}\end{aligned} \tag{78}$$

The symbols $\cancel{\boldsymbol{\rho}_i \otimes \boldsymbol{\omega} \otimes \boldsymbol{\rho}_i}$, $\cancel{\boldsymbol{\rho}_i \otimes \boldsymbol{\omega} \otimes \varDelta\boldsymbol{\rho}_i}$, $\cancel{\varDelta\boldsymbol{\rho}_i \otimes \boldsymbol{\omega} \otimes \boldsymbol{\rho}_i}$ and $\cancel{\varDelta\boldsymbol{\rho}_i \otimes \boldsymbol{\omega} \otimes \varDelta\boldsymbol{\rho}_i}$ denote quantities which have been formally introduced in the previous expression simply to preserve its symmetry of representation and to facilitate the reader in checking the correctness of formula (81). As a matter of fact they do not have to be computed since they are associated with the integral (65) and its discrete counterpart $\mathbf{d}_{\boldsymbol{\rho}}^{\partial_i\Omega} \otimes \boldsymbol{\omega} \otimes \mathbf{d}_{\boldsymbol{\rho}}^{\partial_i\Omega}$ in (68). The computation of this last quantity is addressed in subsection 3.3.

Substituting the previous expressions in (68) and defining

$$\theta_{\boldsymbol{\rho}_i}^P = \frac{\mathbf{C} \cdot \mathbf{D}_{\boldsymbol{\rho}_i\boldsymbol{\omega}}}{2} + \frac{\mathbb{C}}{3} \cdot \left(\mathbb{D}_{\boldsymbol{\omega\omega\rho}_i} + \mathbb{D}_{\boldsymbol{\rho}_i\boldsymbol{\rho}_i\boldsymbol{\omega}}\right) \tag{79}$$

$$\theta_{\varDelta\boldsymbol{\rho}_i}^P = \frac{\mathbf{C} \cdot \mathbf{D}_{\varDelta\boldsymbol{\rho}_i\boldsymbol{\omega}}}{2} + \frac{\mathbb{C}}{3} \cdot \left(\mathbb{D}_{\boldsymbol{\omega\omega}\varDelta\boldsymbol{\rho}_i} + \mathbb{D}_{\boldsymbol{\rho}_i\varDelta\boldsymbol{\rho}_i\boldsymbol{\omega}}\right) \qquad \theta_{\varDelta\boldsymbol{\rho}_i\varDelta\boldsymbol{\rho}_i}^P = \frac{\mathbb{C} \cdot \mathbb{D}_{\varDelta\boldsymbol{\rho}_i\varDelta\boldsymbol{\rho}_i\boldsymbol{\omega}}}{3} \tag{80}$$

we get

$$\begin{aligned}\mathbf{g}_z(\boldsymbol{o}) &= 2G\sum_{i=1}^{n}(\boldsymbol{\rho}_i \cdot \boldsymbol{\rho}_{i+1}^{\perp})\Big\{I_{0i}\Big[a_i(\theta_{\boldsymbol{o}} + \theta_{\boldsymbol{\rho}_i}^O + \theta_{\boldsymbol{\omega}} + \theta_{\boldsymbol{\rho}_i}^P)\Big] + \\ &+ I_{1i}\Big[a_i(\theta_{\varDelta\boldsymbol{\rho}_i}^O + \theta_{\varDelta\boldsymbol{\rho}_i}^P) + b_i(\theta_{\boldsymbol{o}} + \theta_{\boldsymbol{\rho}_i}^O + \theta_{\boldsymbol{\omega}} + \theta_{\boldsymbol{\rho}_i}^P)\Big] + \\ &+ I_{2i}\Big[a_i(\theta_{\varDelta\boldsymbol{\rho}_i\varDelta\boldsymbol{\rho}_i}^O + \theta_{\varDelta\boldsymbol{\rho}_i\varDelta\boldsymbol{\rho}_i}^P) + b_i(\theta_{\varDelta\boldsymbol{\rho}_i}^O + \theta_{\varDelta\boldsymbol{\rho}_i}^P)\Big] + \\ &+ I_{3i}\Big[a_i\theta_{\varDelta\boldsymbol{\rho}_i\varDelta\boldsymbol{\rho}_i\varDelta\boldsymbol{\rho}_i}^O + b_i(\theta_{\varDelta\boldsymbol{\rho}_i\varDelta\boldsymbol{\rho}_i}^O + \theta_{\varDelta\boldsymbol{\rho}_i\varDelta\boldsymbol{\rho}_i}^P)\Big] + I_{4i}b_i\theta_{\varDelta\boldsymbol{\rho}_i\varDelta\boldsymbol{\rho}_i\varDelta\boldsymbol{\rho}_i}^O\Big\}\end{aligned} \tag{81}$$

where $\theta_{\boldsymbol{o}}$ is defined in (13), a_i, b_i in (42), I_{ki} $(k = 0,1,2,3)$ in (57), $\theta^O_{\boldsymbol{\rho}_i}$-$\theta^O_{\Delta\boldsymbol{\rho}_i}$-$\theta^O_{\Delta\boldsymbol{\rho}_i\Delta\boldsymbol{\rho}_i}$- $\theta^O_{\Delta\boldsymbol{\rho}_i\Delta\boldsymbol{\rho}_i\Delta\boldsymbol{\rho}_i}$ in (52)-(55), $\theta_{\boldsymbol{\omega}}$ in (66), $\theta^P_{\boldsymbol{\rho}_i}$-$\theta^P_{\Delta\boldsymbol{\rho}_i}$-$\theta^P_{\Delta\boldsymbol{\rho}_i\Delta\boldsymbol{\rho}_i}$ in (79)-(80).

By eliminating all terms depending explicitly by $\boldsymbol{\omega}$, i.e. $\theta_{\boldsymbol{\omega}}$, $\theta^P_{\boldsymbol{\rho}_i}$, $\theta^P_{\Delta\boldsymbol{\rho}_i}$ and $\theta^P_{\Delta\boldsymbol{\rho}_i\Delta\boldsymbol{\rho}_i}$, it can be easily checked that the previous expression does specialize to (56) when $\boldsymbol{\omega} = \boldsymbol{o}$, i.e. when the gravity anomaly is evaluated at the origin of the reference frame. The previous expression is particularly useful for programming since I_{2i}, I_{3i} and I_{4i} can be expressed as function of I_{0i} and I_{1i} by means of formulas (130), (131) and (132) detailed in Appendix B. The resulting formula is not reported explicitly since it amounts to performing straightforward algebraic manipulations.

To derive an alternative expression of the gravity anomaly which can be conveniently used to check the correct implementation of the more efficient one reported in (81), one can set

$$\iota_{ki} = a_i I_{ki} + b_i I_{(k+1)i} \qquad k = 0,\dots,3 \tag{82}$$

and replace formulas (69)-(72) with

$$d^{\partial_i\Omega}_{\boldsymbol{\rho}} = \iota_{0i} \qquad \mathbf{d}^{\partial_i\Omega}_{\boldsymbol{\rho}} = \iota_{0i}\boldsymbol{\rho}_i + \iota_{1i}\Delta\boldsymbol{\rho}_i \tag{83}$$

$$\mathbf{D}^{\partial_i\Omega}_{\boldsymbol{\rho\rho}} = \iota_{0i}\mathbf{D}_{\boldsymbol{\rho}_i\boldsymbol{\rho}_i} + \iota_{1i}\mathbf{D}_{\boldsymbol{\rho}_i\Delta\boldsymbol{\rho}_i} + \iota_{2i}\mathbf{D}_{\Delta\boldsymbol{\rho}_i\Delta\boldsymbol{\rho}_i} \tag{84}$$

$$\mathbb{D}^{\partial_i\Omega}_{\boldsymbol{\rho\rho\rho}} = \iota_{0i}\mathbb{D}_{\boldsymbol{\rho}_i\boldsymbol{\rho}_i\boldsymbol{\rho}_i} + \iota_{1i}\mathbb{D}_{\boldsymbol{\rho}_i\boldsymbol{\rho}_i\Delta\boldsymbol{\rho}_i} + \iota_{2i}\mathbb{D}_{\boldsymbol{\rho}_i\Delta\boldsymbol{\rho}_i\Delta\boldsymbol{\rho}_i} + \iota_{3i}\mathbb{D}_{\Delta\boldsymbol{\rho}_i\Delta\boldsymbol{\rho}_i\Delta\boldsymbol{\rho}_i} \tag{85}$$

Hence, formula (68) becomes

$$\begin{aligned}
\mathbf{g}_z(\boldsymbol{\omega}) = {} & 2G\sum_{i=1}^{n}\boldsymbol{\rho}_i\cdot\boldsymbol{\rho}^{\perp}_{i+1}\Big\{[\theta_{\boldsymbol{o}}+\theta_{\boldsymbol{\omega}}]\iota_{0i} + \frac{\mathbf{c}}{2}\cdot(\iota_{0i}\boldsymbol{\rho}_i + \iota_{1i}\Delta\boldsymbol{\rho}_i) + \\
& +\mathbf{C}\cdot\Big[\iota_{0i}\Big(\frac{\mathbf{D}_{\boldsymbol{\rho}_i\boldsymbol{\omega}}}{2} + \frac{\mathbf{D}_{\boldsymbol{\rho}_i\boldsymbol{\rho}_i}}{3}\Big) + \iota_{1i}\Big(\frac{\mathbf{D}_{\Delta\boldsymbol{\rho}_i\boldsymbol{\omega}}}{2} + \frac{\mathbf{D}_{\boldsymbol{\rho}_i\Delta\boldsymbol{\rho}_i}}{3}\Big) + \iota_{2i}\frac{\mathbf{D}_{\Delta\boldsymbol{\rho}_i\Delta\boldsymbol{\rho}_i}}{3}\Big] + \\
& +\mathbb{C}\cdot\Big[\iota_{0i}\Big(\frac{\mathbb{D}_{\boldsymbol{\omega\omega\rho}_i}}{2} + \frac{\mathbb{D}_{\boldsymbol{\rho}_i\boldsymbol{\rho}_i\boldsymbol{\omega}}}{3} + \frac{\mathbb{D}_{\boldsymbol{\rho}_i\boldsymbol{\rho}_i\boldsymbol{\rho}_i}}{4}\Big) + \iota_{1i}\Big(\frac{\mathbb{D}_{\boldsymbol{\omega\omega}\Delta\boldsymbol{\rho}_i}}{2} + \frac{\mathbb{D}_{\boldsymbol{\rho}_i\Delta\boldsymbol{\rho}_i\boldsymbol{\omega}}}{3} + \frac{\mathbb{D}_{\boldsymbol{\rho}_i\boldsymbol{\rho}_i\Delta\boldsymbol{\rho}_i}}{4}\Big) + \\
& \quad + \iota_{2i}\Big(\frac{\mathbb{D}_{\Delta\boldsymbol{\rho}_i\Delta\boldsymbol{\rho}_i\boldsymbol{\omega}}}{3} + \frac{\mathbb{D}_{\boldsymbol{\rho}_i\Delta\boldsymbol{\rho}_i\Delta\boldsymbol{\rho}_i}}{4}\Big) + \iota_{3i}\frac{\mathbb{D}_{\Delta\boldsymbol{\rho}_i\Delta\boldsymbol{\rho}_i\Delta\boldsymbol{\rho}_i}}{4}\Big]\Big\}
\end{aligned} \tag{86}$$

a formula which can be further elaborated upon by expressing I_{2i}, I_{3i} and I_{4i} as function of I_{0i} and I_{1i} in the formulas for ι_{2i}, ι_{3i} and ι_{4i}.

3.3 Evaluation of the third-order tensor $\mathbf{d}^{\partial_i\Omega}_{\boldsymbol{\rho}}\otimes\boldsymbol{\omega}\otimes\mathbf{d}^{\partial_i\Omega}_{\boldsymbol{\rho}}$

We have denoted by the symbol $\mathbf{d}^{\partial_i\Omega}_{\boldsymbol{\rho}}\otimes\boldsymbol{\omega}\otimes\mathbf{d}^{\partial_i\Omega}_{\boldsymbol{\rho}}$ in (68) the third-order tensor

$$\mathbf{d}^{\partial_i\Omega}_{\boldsymbol{\rho}}\otimes\boldsymbol{\omega}\otimes\mathbf{d}^{\partial_i\Omega}_{\boldsymbol{\rho}} = \int_0^1 \frac{[\boldsymbol{\rho}(\lambda_i)\cdot\boldsymbol{\kappa}_z]\boldsymbol{\rho}(\lambda_i)\otimes\boldsymbol{\omega}\otimes\boldsymbol{\rho}(\lambda_i)}{\boldsymbol{\rho}(\lambda_i)\cdot\boldsymbol{\rho}(\lambda_i)}d\lambda_i \tag{87}$$

As a matter of fact the tensor to evaluate is the rank-two tensor $\mathbf{D}^{\partial_i\Omega}_{\boldsymbol{\rho\rho}}$ since its components have to be suitably combined with those of $\boldsymbol{\omega}$ in order to compute (87). In turn this depends upon the rule which is adopted to define the matrix associated with a third-order tensor, a rule which usually depends upon the adopted programming language. For instance, extending the rule defined in (11) to three arbitrary vectors **t**, **v** and **w** one obtains

$$\mathbf{t} \otimes (\mathbf{v} \otimes \mathbf{w}) = \begin{bmatrix} t_1 v_1 w_1 & t_1 v_1 w_2 \\ t_1 v_2 w_1 & t_1 v_2 w_2 \\ \hline t_2 v_1 w_1 & t_2 v_1 w_2 \\ t_2 v_2 w_1 & t_2 v_2 w_2 \end{bmatrix} \tag{88}$$

The products $t_1 w_1$, $t_1 w_2$ etc. are the components of the tensor $\mathbf{t} \otimes \mathbf{w}$ which plays the role of the tensor $\mathbf{D}^{\partial_i \Omega}_{\boldsymbol{\rho}\boldsymbol{\rho}}$, i.e. the one to be actually computed.

Accordingly, we can define the matrix associated with $\mathbf{d}^{\partial_i \Omega}_{\boldsymbol{\rho}} \otimes \boldsymbol{\omega} \otimes \mathbf{d}^{\partial_i \Omega}_{\boldsymbol{\rho}}$ as

$$[\mathbf{d}^{\partial_i \Omega}_{\boldsymbol{\rho}} \otimes \boldsymbol{\omega} \otimes \mathbf{d}^{\partial_i \Omega}_{\boldsymbol{\rho}}] = \begin{bmatrix} \omega_1 [\mathbf{D}^{\partial_i \Omega}_{\boldsymbol{\rho}\boldsymbol{\rho}}]_{11} & \omega_1 [\mathbf{D}^{\partial_i \Omega}_{\boldsymbol{\rho}\boldsymbol{\rho}}]_{12} \\ \omega_2 [\mathbf{D}^{\partial_i \Omega}_{\boldsymbol{\rho}\boldsymbol{\rho}}]_{11} & \omega_2 [\mathbf{D}^{\partial_i \Omega}_{\boldsymbol{\rho}\boldsymbol{\rho}}]_{12} \\ \hline \omega_1 [\mathbf{D}^{\partial_i \Omega}_{\boldsymbol{\rho}\boldsymbol{\rho}}]_{21} & \omega_1 [\mathbf{D}^{\partial_i \Omega}_{\boldsymbol{\rho}\boldsymbol{\rho}}]_{22} \\ \omega_2 [\mathbf{D}^{\partial_i \Omega}_{\boldsymbol{\rho}\boldsymbol{\rho}}]_{21} & \omega_2 [\mathbf{D}^{\partial_i \Omega}_{\boldsymbol{\rho}\boldsymbol{\rho}}]_{22} \end{bmatrix} \tag{89}$$

where $[\mathbf{D}^{\partial_i \Omega}_{\boldsymbol{\rho}\boldsymbol{\rho}}]_{ij}$ denotes the ij entry of the matrix associated with $\mathbf{D}^{\partial_i \Omega}_{\boldsymbol{\rho}\boldsymbol{\rho}}$.

4 Ineffective singularities of the algebraic expressions of the gravity anomaly

It has already been shown that the analytical expression (31) of the gravity anomaly is singularity-free in the sense that its expression holds rigorously whatever is the position of the point O with respect to Ω. The same property holds true for the expression (67) referred to an arbitrary point P. However, the algebraic counterparts of (31) and (67), which are provided by formulas (56) and (81), respectively, still hide some singularities.

They are associated with the expression of the integrals I_{ki}, provided in (57), since some special positions of the generic edge of $\partial\Omega$ with respect to the observation point can make the denominator of (57) vanish. However, we are going to prove that such singularities are ineffective from the computational point of view since they can be actually ignored when evaluating the i-th addend of the sums (56) and (81).

To fully understand this point let us first notice that the opposite of the discriminant Δ_i of the quadratic function at the denominator in (57) is always non-negative, being

$$\Delta_i = p_i u_i - q_i^2 = (\boldsymbol{\rho}_{i+1} \cdot \boldsymbol{\rho}_{i+1})(\boldsymbol{\rho}_i \cdot \boldsymbol{\rho}_i) - (\boldsymbol{\rho}_i \cdot \boldsymbol{\rho}_{i+1})^2 \geq 0 \tag{90}$$

by virtue of the Cauchy-Schwarz inequality (Tang, 2006). The quantity Δ_i can vanish, making undefined the integral I_{ki} in (57), if and only if either $\boldsymbol{\rho}_i(\boldsymbol{\rho}_{i+1}) = \boldsymbol{o}$ or $\boldsymbol{\rho}_i$ and $\boldsymbol{\rho}_{i+1}$ are parallel. In turn this happens when the observation point does belong to the line containing the i-th edge. Accordingly, if $\Delta_i > 0$, formulas (124) and (125) specialize to

$$I_{0i} = \frac{1}{\sqrt{\Delta_i}} \Big[\arctan \frac{\boldsymbol{\rho}_{i+1} \cdot \Delta\boldsymbol{\rho}_i}{\sqrt{\Delta_i}} - \arctan \frac{\boldsymbol{\rho}_i \cdot \Delta\boldsymbol{\rho}_i}{\sqrt{\Delta_i}} \Big] \tag{91}$$

and

$$I_{1i} = \frac{1}{\Delta\boldsymbol{\rho}_i \cdot \Delta\boldsymbol{\rho}_i} \Big[\frac{1}{2} \log \frac{\boldsymbol{\rho}_{i+1} \cdot \boldsymbol{\rho}_{i+1}}{\boldsymbol{\rho}_i \cdot \boldsymbol{\rho}_i} - (\boldsymbol{\rho}_i \cdot \Delta\boldsymbol{\rho}_i) I_{0i} \Big] \tag{92}$$

respectively. Furthermore, formulas (130), (131) and (132) can be used to evaluate I_{2i}, I_{3i} and I_{4i}.

Clearly, the previous expressions become singular if $\Delta_i = 0$, i.e. when the i-th edge does belong to a line containing the observation point. Nevertheless, we shall prove that the contribution of the i-th edge to the gravity anomaly is zero. Hence, from the computational point of view, it is possible to skip the evaluation of the i-th addend in formula (56) whenever the i-th edge does belong to a line containing O. The same property can be invoked for formulas (81) and (86) whenever the i-th edge does belong to a line containing the arbitrary point P at which the gravity anomaly is required. The conditions stated above do hold when $\boldsymbol{\rho}_i = \boldsymbol{o}$ or $\boldsymbol{\rho}_{i+1} = \boldsymbol{o}$ or $\boldsymbol{\rho}_i$ is parallel to $\boldsymbol{\rho}_{i+1}$. These three cases will be addressed separately in the sequel.

4.1 Specialization of the line integrals (35)-(37) to the case $\boldsymbol{\rho}_i = \boldsymbol{o}$

Recalling (41) the parameterization of the i-th edge becomes

$$\boldsymbol{\rho}(\lambda_i) = \lambda_i \boldsymbol{\rho}_{i+1} \tag{93}$$

so that

$$\boldsymbol{\rho}(\lambda_i) \cdot \boldsymbol{\kappa}_z = \lambda_i \boldsymbol{\rho}_{i+1} \cdot \boldsymbol{\kappa}_z = b_i \lambda_i \tag{94}$$

and

$$\boldsymbol{\rho}(\lambda_i) \cdot \boldsymbol{\rho}(\lambda_i) = \lambda_i^2 \boldsymbol{\rho}_{i+1} \cdot \boldsymbol{\rho}_{i+1} = p_i \lambda_i^2 \tag{95}$$

Accordingly, we get from (35)-(37)

$$d_{\boldsymbol{\rho}}^{\partial_i \Omega} = \frac{b_i}{p_i} \int_0^1 \frac{d\lambda_i}{\lambda_i} = \frac{b_i}{p_i} \lim_{\varepsilon \to 0} [\log \lambda_i]_{\varepsilon}^1 \tag{96}$$

which is singular at $\lambda_i = 0$, and

$$\mathbf{d}_{\boldsymbol{\rho}}^{\partial_i \Omega} = \frac{b_i}{p_i} \boldsymbol{\rho}_{i+1} \qquad \mathbf{D}_{\boldsymbol{\rho\rho}}^{\partial_i \Omega} = \frac{1}{2} \frac{b_i}{p_i} \boldsymbol{\rho}_{i+1} \otimes \boldsymbol{\rho}_{i+1} \qquad \mathbb{D}_{\boldsymbol{\rho\rho\rho}}^{\partial_i \Omega} = \frac{1}{3} \frac{b_i}{p_i} \boldsymbol{\rho}_{i+1} \otimes \boldsymbol{\rho}_{i+1} \otimes \boldsymbol{\rho}_{i+1} \tag{97}$$

However, $d_{\boldsymbol{\rho}}^{\partial_i \Omega}$ in formulas (40) and (68), and hence the logarithm in (96), is scaled by $\boldsymbol{\rho}_i \cdot \boldsymbol{\rho}_{i+1}^{\perp}$. Setting $\varepsilon = |\boldsymbol{\rho}_i|$, we infer that

$$\lim_{\varepsilon \to 0} (\boldsymbol{\rho}_i \cdot \boldsymbol{\rho}_{i+1}^{\perp}) I_{0i} = \lim_{\varepsilon \to 0} \varepsilon \frac{b_i}{p_i} \log \varepsilon = 0 \tag{98}$$

since the logarithm tends to infinite with an arbitrarily low degree. In addition, being $\mathbf{d}_{\boldsymbol{\rho}}^{\partial_i \Omega}$, $\mathbf{D}_{\boldsymbol{\rho\rho}}^{\partial_i \Omega}$ and $\mathbb{D}_{\boldsymbol{\rho\rho\rho}}^{\partial_i \Omega}$ finite, we ultimately infer that the contribution of the i-th edge to the expressions (56), (81) and (86) of the gravity anomaly is zero.

4.2 Specialization of the line integrals (35)-(37) to the case $\boldsymbol{\rho}_{i+1} = \boldsymbol{o}$

In this case the i-th edge is parameterized in the form

$$\boldsymbol{\rho}(\lambda_i) = \eta_i \boldsymbol{\rho}_i = (1-\lambda_i)\boldsymbol{\rho}_i \qquad 0 \le \eta \le 1 \tag{99}$$

Hence

$$\boldsymbol{\rho}(\lambda_i) \cdot \boldsymbol{\kappa}_z = \eta_i \boldsymbol{\rho}_i \cdot \boldsymbol{\kappa}_z = a_i \eta_i \tag{100}$$

and

$$\boldsymbol{\rho}(\lambda_i) \cdot \boldsymbol{\rho}(\lambda_i) = \eta_i^2 \boldsymbol{\rho}_i \cdot \boldsymbol{\rho}_i = u_i \eta_i^2 \tag{101}$$

Being $d\lambda_i = -d\eta_i$ one has

$$d_{\boldsymbol{\rho}}^{\partial_i \Omega} = -\frac{a_i}{u_i} \int_1^0 \frac{d\eta_i}{\eta_i} = \frac{a_i}{u_i} \lim_{\varepsilon \to 0} [\log \lambda_i]_{\varepsilon}^1 \tag{102}$$

$$\mathbf{d}_{\boldsymbol{\rho}}^{\partial_i \Omega} = \frac{a_i}{u_i} \boldsymbol{\rho}_i \qquad \mathbf{D}_{\boldsymbol{\rho}\boldsymbol{\rho}}^{\partial_i \Omega} = \frac{1}{2} \frac{a_i}{u_i} \boldsymbol{\rho}_i \otimes \boldsymbol{\rho}_i \qquad \mathbb{D}_{\boldsymbol{\rho}\boldsymbol{\rho}\boldsymbol{\rho}}^{\partial_i \Omega} = \frac{1}{3} \frac{a_i}{u_i} \boldsymbol{\rho}_i \otimes \boldsymbol{\rho}_i \otimes \boldsymbol{\rho}_i \tag{103}$$

Hence, we can repeat the considerations developed in the previous subsection, by exchanging the role of $\boldsymbol{\rho}_i$ and $\boldsymbol{\rho}_{i+1}$, and conclude that the contribution of the i-th edge to the expressions (56), (81) and (86) of the gravity anomaly vanishes.

4.3 Specialization of the line integrals (35)-(37) to the case $\boldsymbol{\rho}_i \| \boldsymbol{\rho}_{i+1}$

In this case we can set $\boldsymbol{\rho}_{i+1} = \beta_i \boldsymbol{\rho}_i$ with $0 < \beta_i = |\boldsymbol{\rho}_{i+1}|/|\boldsymbol{\rho}_i|$ and parameterize the i-th edge as

$$\boldsymbol{\rho}[\lambda_i(\xi_i)] = \xi_i \boldsymbol{\rho}_i \tag{104}$$

where

$$\xi_i = 1 + \lambda_i(\beta_i - 1) \qquad 1 \le \xi_i \le \beta_i \tag{105}$$

and it has been assumed $\beta_i > 1$. As it will be apparent in the sequel, the case $\beta_i < 1$ does not modify the final result. Being also

$$\boldsymbol{\rho}(\lambda_i) \cdot \boldsymbol{\kappa}_z = \xi_i \boldsymbol{\rho}_i \cdot \boldsymbol{\kappa}_z = a_i \xi_i \tag{106}$$

and

$$\boldsymbol{\rho}(\lambda_i) \cdot \boldsymbol{\rho}(\lambda_i) = p_i \xi_i^2 \tag{107}$$

and $d\xi_i = d\lambda_i(\beta_i - 1)$ we now have

$$d_{\boldsymbol{\rho}}^{\partial_i \Omega} = \frac{a_i}{p_i(\beta_i - 1)} \int_1^{\beta_i} \frac{d\xi_i}{\xi_i} = \frac{a_i}{p_i} \frac{\log \beta_i}{\beta_i - 1} \tag{108}$$

$$\mathbf{d}_{\boldsymbol{\rho}}^{\partial_i \Omega} = \frac{a_i}{p_i} \boldsymbol{\rho}_i \qquad \mathbf{D}_{\boldsymbol{\rho}\boldsymbol{\rho}}^{\partial_i \Omega} = \frac{1}{2} \frac{a_i}{p_i} (\beta_i + 1) \boldsymbol{\rho}_i \otimes \boldsymbol{\rho}_i \qquad \mathbb{D}_{\boldsymbol{\rho}\boldsymbol{\rho}\boldsymbol{\rho}}^{\partial_i \Omega} = \frac{1}{3} \frac{a_i}{p_i} \frac{\beta_i^3 - 1}{\beta_i - 1} \boldsymbol{\rho}_i \otimes \boldsymbol{\rho}_i \otimes \boldsymbol{\rho}_i \tag{109}$$

The four integrals above are well defined but are scaled by the quantity $\boldsymbol{\rho}_i \cdot \boldsymbol{\rho}_{i+1}^{\perp}$ which is zero by hypothesis. Hence, recalling formulas (40) and (68), the i-th edge does not give any contribution to the sum in (56), (81) and (86). In conclusion, it has been proved that, whenever $\boldsymbol{\rho}_i \cdot \boldsymbol{\rho}_{i+1}^{\perp} = 0$, which is equivalent to state $\boldsymbol{\rho}_i = 0$ or $\boldsymbol{\rho}_{i+1} = 0$ or $\boldsymbol{\rho}_i \| \boldsymbol{\rho}_{i+1}$, the computation of the i-th addend of the sum in (56), (81) and (86) can be skipped. Clearly, from the numerical point of view, the analytical condition $\boldsymbol{\rho}_i \cdot \boldsymbol{\rho}_{i+1}^{\perp} = 0$ is replaced by $\|\boldsymbol{\rho}_i \cdot \boldsymbol{\rho}_{i+1}^{\perp}\| \le tol$ where tol is a machine-dependent numerical tolerance.

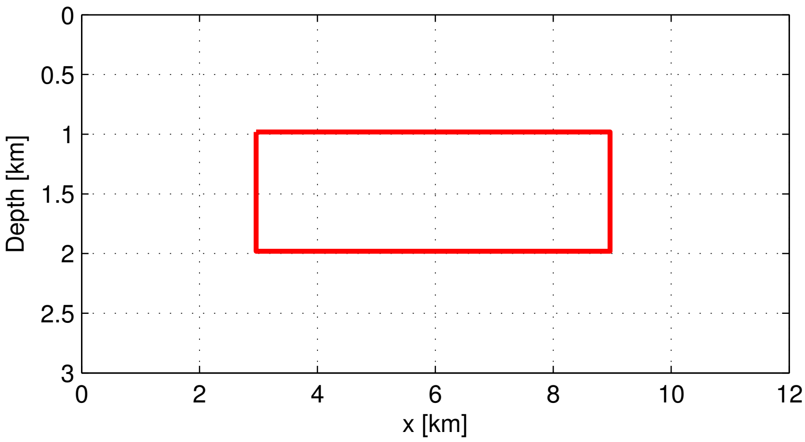

Fig. 3 2-D rectangular domain, derived from Rao (1986), with density contrast given by (110)

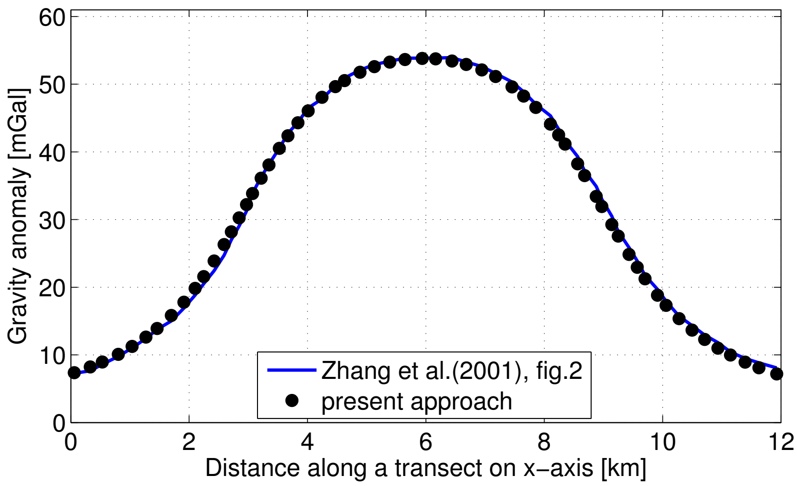

Fig. 4 Comparison between the results of the present approach and those in Zhang et al (2001) for the domain in Fig. 3

5 Numerical examples

The formulas illustrated in the previous sections have been coded in a Matlab program in order to check their correctness and robustness. They have been applied to model tests and case studies derived from the specialized literature. In particular the density contrast has been assumed to vary separately along the horizontal and the vertical directions or along both of them. In all examples the density contrast is expressed in units grams per cubic centimeter while distances are expressed in kilometers; the value of the gravitational constant G is $6,67259\,10^{-11} m^3 kg^{-1} s^{-2}$.

For all the examples we include a graphycal and a tabular comparison between our results and those alrady published in the literature, although these last ones have been inferred, to the best of the author's expertise, from the diagrams in which they have been originally

Table 1 Numerical values of the gravity anomaly (mGal) in fig. 4: a) computed in this paper (CT=0,07923s); b) derived from the diagram in Zhang et al (2001)

x(km)	0,0	0,33	0,53	0,80	1,04	1,27	1,46	1,70	1,91	2,10	2,25
a)	7,206	8,215	8,954	10,092	11,255	12,622	13,912	15,823	17,797	19,831	21,578
b)	7,280	7,649	8,606	9,784	11,036	12,434	13,759	15,010	16,924	18,836	20,529
x(km)	2,42	2,59	2,71	2,84	2,97	3,07	3,22	3,35	3,52	3,67	3,84
a)	23,885	26,295	28,179	30,241	32,218	33,843	36,118	38,081	40,525	42,384	44,308
b)	22,441	24,722	27,002	29,062	31,268	33,916	36,270	38,182	40,536	42,743	44,362
x(km)	4,01	4,25	4,47	4,62	4,89	5,13	5,39	5,65	5,94	6,16	6,44
a)	46,073	48,065	49,638	50,528	51,761	52,606	53,256	53,643	53,809	53,741	53,420
b)	46,495	47,820	49,807	50,911	52,089	52,899	53,415	53,858	53,860	53,861	53,937
x(km)	6,68	6,94	7,18	7,46	7,65	7,86	8,10	8,24	8,35	8,56	8,68
a)	52,918	52,109	51,134	49,612	48,255	46,572	44,105	42,511	41,142	38,233	36,500
b)	53,276	52,616	51,588	50,340	48,870	47,033	45,344	43,359	41,669	39,317	37,186
x(km)	8,88	8,97	9,14	9,25	9,43	9,57	9,70	9,91	10,06	10,28	10,50
a)	33,431	31,919	29,254	27,554	24,851	22,939	21,255	18,815	17,323	15,355	13,672
b)	34,907	32,996	30,497	28,218	25,867	23,882	21,751	19,693	17,929	15,725	14,329
x(km)	10,71	10,94	11,15	11,39	11,63	12,00					
a)	12,278	11,001	9,973	8,938	8,103	6,996					
b)	12,933	11,832	10,436	9,482	8,821	8,088					

reported. We also include the computing time (CT) obtained by running the Matlab code on a INTEL CORE2 PC with 16Gb of RAM and a i7-4700HQ CPU having clock speed of 2,40 GHz. They can be useful to allow for a comparison with computations carried out by using different methods or with more complex modellings, e.g. those reqired to evaluate the gravitational effects of an arbitrary volumetric mass layer in which a laterally varying radial density change has been assumed (Tenzer et al, 2012a,b,c).

The model test in fig. 3 is a 2D rectangular cylinder at a depth of 1km, 6 km wide and 1km high; it has been first considered by Rao (1986), and subsequently by Zhang et al (2001), by assuming a density contrast given by

$$\theta(z) = 1.54 + 0.24z - 0.035z^2 \tag{110}$$

Fig. 4 shows a perfect agreement between the solid line, representing jointly the results by Rao (1986) and Zhang et al (2001), and the dotted line which has been computed by means of the proposed approach. Each point in the figure represents the gravity anomaly associated with a position of the observation point having as coordinates $z = 0$ and an abscissa x equal to that of the plotted point.

The second example, shown in fig. 5, has been first addressed by García-Abdeslem et al (2005b) and later considered in Zhou (2008). It refers to the Sebastián Vizcaíno Basin in Mexico for which the density contrast has been assumed in the form

$$\theta(z) = -0.7 + 2.548 * 10^{-4} z - 2.73 * 10^{-8} z^2 \tag{111}$$

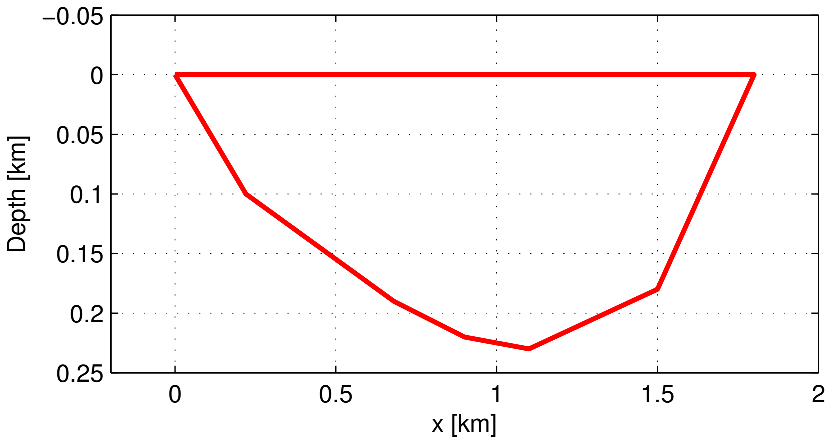

Fig. 5 Domain derived from García-Abdeslem et al (2005b) with density contrast given by (111)

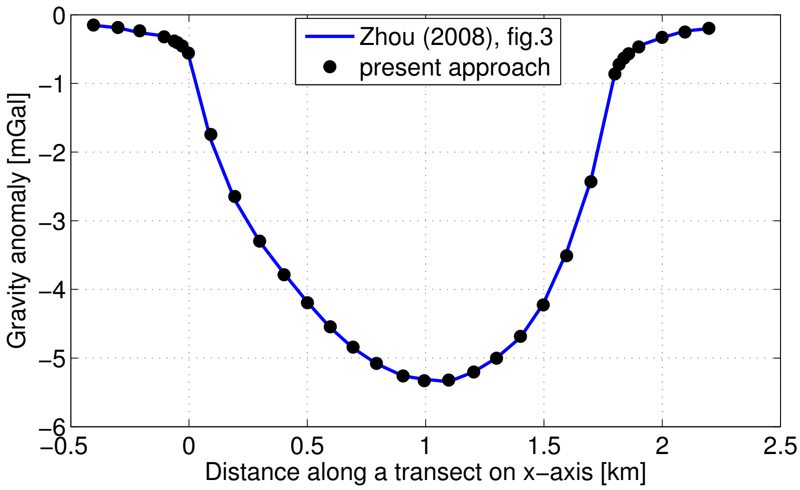

Fig. 6 Comparison between the results of the present approach and those in Zhou (2008) for the domain in Fig. 5

where z is expressed in meters. The gravity anomaly along a transect on the x-axis is shown in fig. 6 and successfully compared with that computed in Zhou (2008) by two distinct methodologies named Line-Integral (LI) with arctangent kernel and density integrated LI. In both methodologies Zhou evaluated the resulting integrals by the Gauss-Legendre quadrature method.

Fig. 7 illustrates an elongated segment valley first considered by Murthy and Rao (1979) and later analyzed by Zhang et al (2001). The density contrast is given by

$$\theta(z) = -0.55 + 2 * 10^{-4} z \tag{112}$$

where z is expressed in meters. Fig. 8 shows the comparison of the gravity anomaly computed by different procedures, i.e. the one presented in Zhang et al (2001), the two methodologies quoted above by Zhou (2008) and that contributed in the present paper.

Table 2 Numerical values of the gravity anomaly (mGal) in fig. 6: a) computed in this paper (CT=0,07081s); b) derived from the diagram in Zhou (2008)

x(km)	-0,40	-0,30	-0,21	-0,11	-0,06	-0,05	-0,03	0,00	0,09	0,19	0,30
a)	-0,150	-0,186	-0,233	-0,322	-0,382	-0,407	-0,454	-0,557	-1,743	-2,647	-3,297
b)	-0,155	-0,191	-0,262	-0,310	-0,370	-0,394	-0,429	-0,584	-1,825	-2,696	-3,304
x(km)	0,40	0,50	0,60	0,69	0,79	0,90	0,99	1,10	1,20	1,30	1,40
a)	-3,787	-4,195	-4,545	-4,841	-5,078	-5,260	-5,331	-5,320	-5,203	-5,002	-4,684
b)	-3,769	-4,187	-4,557	-4,855	-5,082	-5,260	-5,308	-5,344	-5,201	-4,998	-4,700
x(km)	1,50	1,60	1,70	1,80	1,82	1,84	1,86	1,90	2,00	2,10	2,20
a)	-4,226	-3,511	-2,432	-0,863	-0,724	-0,634	-0,568	-0,468	-0,330	-0,252	-0,199
b)	-4,211	-3,459	-2,410	-0,859	-0,728	-0,632	-0,561	-0,453	-0,334	-0,239	-0,203

Table 3 Numerical values of the gravity anomaly (mGal) in fig. 8: a) computed in this paper (CT=0,04594s); b) derived from the diagram in Zhou (2008); c) derived from the diagram in Zhang et al (2001)

x(km)	0,02	0,49	1,02	1,47	2,03	2,49	2,99	3,54	3,99	4,50	5,01
a)	-0,413	-0,460	-0,524	-0,591	-0,695	-0,803	-0,959	-1,192	-1,475	-1,982	-3,356
b)	-0,513	-0,512	-0,511	-0,556	-0,648	-0,787	-0,879	-1,018	-1,297	-1,669	-2,414
c)	-0,373	-0,279	-0,184	-0,230	-0,228	-0,321	-0,506	-0,878	-1,203	-1,669	-2,414
x(km)	5,51	6,00	6,49	6,99	7,55	8,01	8,51	8,99	9,51	10,02	10,51
a)	-8,660	-12,355	-15,284	-17,693	-19,732	-20,975	-21,988	-22,628	-23,032	-23,131	-22,950
b)	-6,517	-10,014	-13,231	-16,215	-18,639	-20,410	-21,669	-22,414	-22,879	-22,971	-22,877
c)	-6,517	-9,874	-13,605	-16,495	-18,127	-20,411	-21,716	-22,601	-22,879	-22,971	-22,690
x(km)	11,00	11,53	11,98	12,49	13,02	13,51	14,04	14,48	14,99	15,48	16,02
a)	-22,482	-21,621	-20,505	-18,744	-16,222	-13,239	-9,781	-6,744	-2,616	-1,701	-1,287
b)	-22,456	-21,522	-20,308	-18,674	-16,248	-13,122	-9,902	-6,543	-2,484	-1,643	-1,222
c)	-21,989	-21,056	-19,749	-18,022	-15,502	-12,749	-9,530	-6,917	-4,118	-2,858	-2,298
x(km)	16,53	17,02	17,51	17,95	18,51	19,02	19,51	20,03			
a)	-1,040	-0,868	-0,739	-0,648	-0,555	-0,488	-0,434	-0,386			
b)	-0,941	-0,753	-0,705	-0,564	-0,517	-0,422	-0,374	-0,373			
c)	-1,597	-0,942	-0,568	-0,427	-0,286	-0,238	-0,376	-0,466			

Fig. 9 illustrates a case analyzed by Martín-Atienza and García-Abdeslem (1999), Zhou (2009a, 2010) in which the density contrast varies only along the horizontal position

$$\theta(z) = 0.5 + 2 * 10^{-5} x - 2 * 10^{-8} x^2 \tag{113}$$

The gravity anomaly, calculated along a transect on the x-axis, is shown in fig 10 where our results are compared with those obtained by Zhou (2010). These last results had been previously compared by Zhou with those based on the LI method with logarithmic kernel, previously contributed in Zhou (2009a), and the original results by Martín-Atienza and García-Abdeslem (1999).

The last numerical example, shown in fig. 11, refers to a case first studied by Martín-Atienza and García-Abdeslem (1999) and later re-examined in Zhou (2009a). The geometry

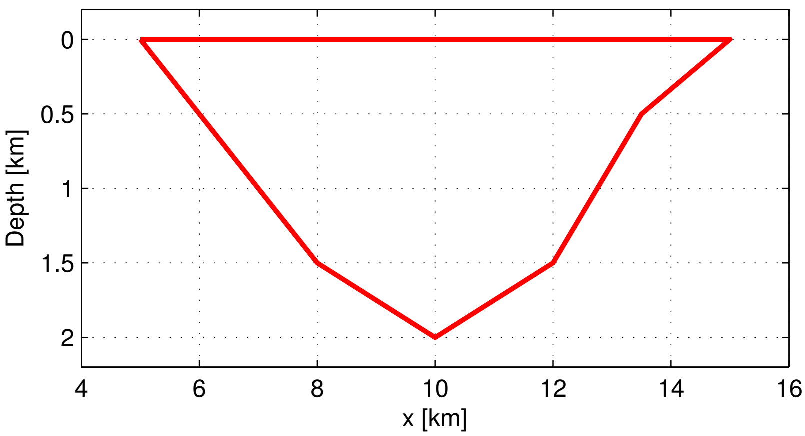

Fig. 7 Domain derived from Murthy and Rao (1979) with density contrast given by (112)

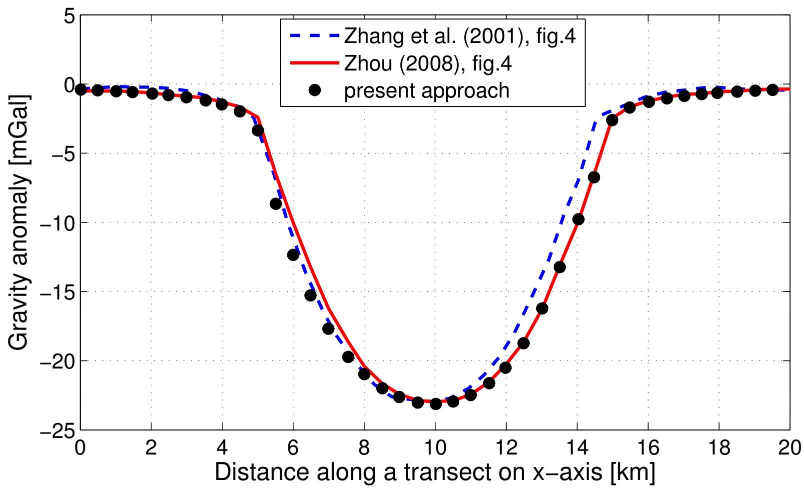

Fig. 8 Comparison between the results of the present approach and those in Zhang et al (2001) and Zhou (2008) for the domain in Fig. 7

in fig. 11 refers to folded and overturned strata in a sedimentary basin in which the density contrast varies simultaneously along the horizontal and vertical directions

$$\theta(x,z) = -0.7 - 5*10^{-8}xz + 4*10^{-8}x^2 + 6*10^{-8}z^2 \tag{114}$$

The boundary of the body has been approximated by a 26-sided polygon and the gravity anomaly has been computed at 41 stations. The high number of polygon vertices and the more complex density contrast function exlain the computing time of $0,32681s$ which is considerably higher than those experienced in previous examples. Figure 12 superimposes our results with those obtained by Martín-Atienza and García-Abdeslem (1999), the seminumerical LI method by Zhou (2009a) and the analytical method in Zhou (2010).

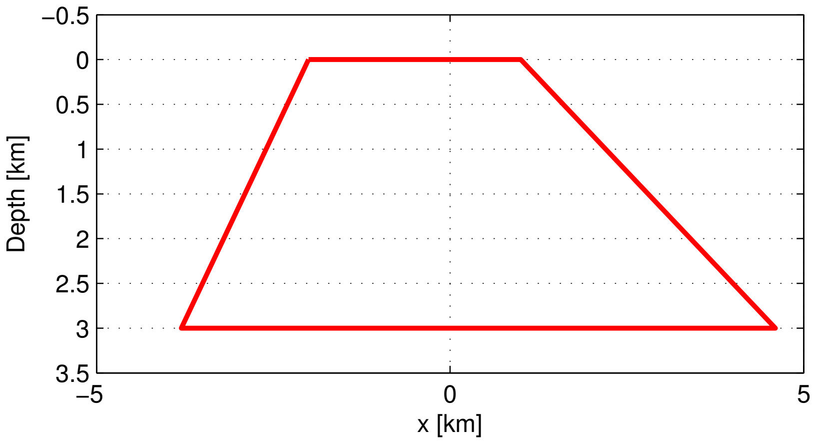

Fig. 9 Domain derived from Martín-Atienza and García-Abdeslem (1999) with density contrast given by (113)

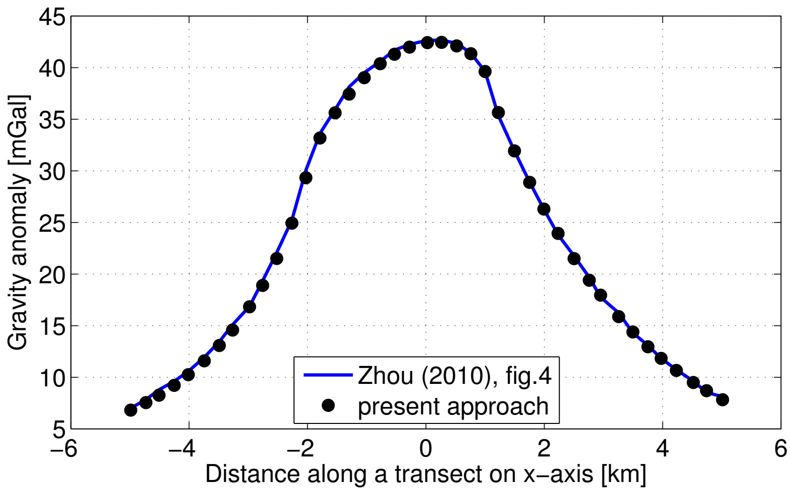

Fig. 10 Comparison between the results of the present approach and those in Zhou (2010) for the domain in Fig. 9

5.1 Error analysis

It is interesting to consider the susceptibility of the formulas derived in the paper to numerical rounding error. As shown in Holstein and Ketteridge (1996) this depends on the target aspect ratio $\gamma = \alpha/\delta$ where α is the typical linear dimension of the target and δ its typical distance from the observation point. For 2D bodies the anomaly calculation (6) is governed by an area integral weighted by the density contrast, the vertical component of the position vector, proportional to δ, and the inverse square law factor, proportional to $1/\delta^2$.

The density contrast functions considered in the previous examples show that $\theta(\boldsymbol{\rho})$ is obtained as sum of separate terms having substantially the same order of magnitude as the

Table 4 Numerical values of the gravity anomaly (mGal) in fig. 10: a) computed in this paper (CT=0,05527s); b) derived from the diagram in Zhou (2010)

x(km)	-4,99	-4,73	-4,51	-4,25	-4,01	-3,74	-3,49	-3,27	-2,98	-2,76	-2,52
a)	6,804	7,533	8,261	9,212	10,239	11,587	13,068	14,564	16,820	18,889	21,502
b)	7,005	7,826	8,784	9,605	10,563	11,933	13,441	15,086	16,868	19,337	22,081

x(km)	-2,26	-2,03	-1,79	-1,53	-1,30	-1,04	-0,77	-0,53	-0,28	0,03	0,27
a)	24,929	29,326	33,170	35,616	37,440	39,031	40,378	41,290	41,983	42,419	42,443
b)	25,237	30,042	33,610	35,941	38,136	39,506	40,601	41,697	42,243	42,651	42,648

x(km)	0,52	0,76	1,00	1,22	1,50	1,75	1,99	2,23	2,51	2,76	2,95
a)	42,109	41,351	39,618	35,642	31,930	28,880	26,295	23,931	21,488	19,396	17,950
b)	42,369	41,404	39,615	35,354	31,916	28,891	26,278	23,802	21,738	19,674	17,748

x(km)	3,26	3,50	3,75	3,98	4,23	4,52	4,74	5,01
a)	15,865	14,384	12,955	11,823	10,658	9,495	8,690	7,820
b)	16,233	14,306	13,067	11,827	10,725	9,622	8,520	8,104

Table 5 Numerical values of the gravity anomaly (mGal) in fig. 12: a) computed in this paper (CT=0,32681s); b) derived from the diagram in Zhou (2010)

x(km)	-5,00	-4,76	-4,54	-4,27	-4,00	-3,76	-3,51	-3,24	-3,03	-2,78	-2,52
a)	-4,362	-4,814	-5,323	-6,136	-7,582	-9,554	-12,092	-15,103	-17,544	-20,635	-23,758
b)	-4,286	-4,762	-5,714	-6,349	-7,619	-9,841	-12,222	-15,238	-17,937	-21,111	-24,286

x(km)	-2,29	-2,00	-1,78	-1,54	-1,27	-1,02	-0,75	-0,52	-0,29	-0,02	0,22
a)	-26,660	-30,049	-32,574	-35,140	-37,836	-40,136	-42,296	-43,835	-45,228	-46,468	-47,250
b)	-26,984	-30,476	-32,857	-35,556	-38,095	-40,159	-42,222	-43,968	-45,238	-46,825	-47,302

x(km)	0,48	0,71	0,97	1,22	1,46	1,73	1,94	2,24	2,48	2,73	2,97
a)	-47,750	-47,900	-47,712	-47,163	-46,320	-44,985	-43,695	-41,404	-39,269	-36,692	-34,020
b)	-47,778	-47,937	-47,619	-47,302	-46,191	-44,762	-43,175	-41,111	-38,730	-36,191	-33,492

x(km)	3,19	3,46	3,70	3,97	4,19	4,48	4,73	5,00
a)	-31,326	-27,840	-24,622	-20,910	-17,913	-14,528	-12,779	-11,074
b)	-30,318	-26,984	-23,492	-20,000	-16,667	-13,968	-12,064	-10,476

constant term θ_o. Nevertheless one has to consider separately the integrals (17)-(18) and compute their one-dimensional counterparts (28)-(29).

In particular, we have

$$d_\rho^\Omega \approx O(\alpha) = O(\delta\gamma) \qquad \mathbf{d}_\rho^\Omega \approx O(\delta\alpha) = O(\delta^2\gamma) \tag{115}$$

and

$$\mathbf{D}_{\rho\rho}^\Omega \approx O(\delta^2\alpha) = O(\delta^3\gamma) \qquad \mathbb{D}_{\rho\rho\rho}^\Omega \approx O(\delta^3\alpha) = O(\delta^4\gamma) \tag{116}$$

where $\approx$ means "has order of magnitude equal to".

Thus, when computed in a finite floating point precision ϵ, the rounding error $O(\delta^k\gamma\epsilon)$, $k = 1, \ldots 4$, progressively increases as the target distance δ increases relative to the target

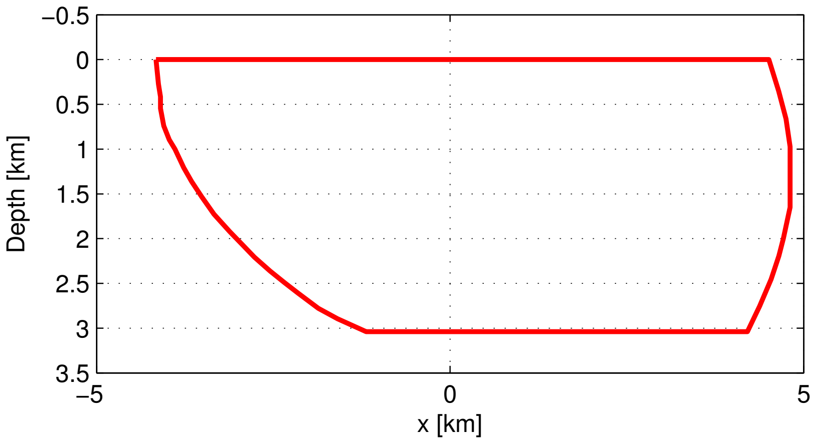

Fig. 11 Domain derived from Martín-Atienza and García-Abdeslem (1999) with density contrast given by (114)

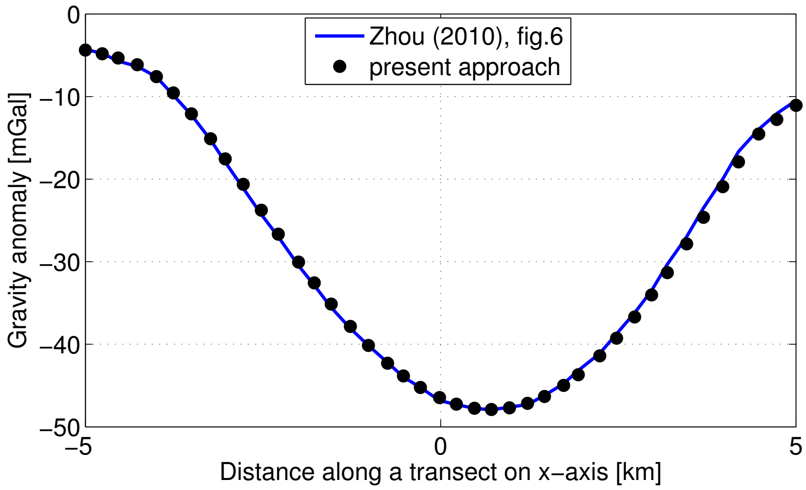

Fig. 12 Comparison between the results of the present approach and those in Zhou (2010) for the domain in Fig. 11

size α. However, as shown in the previous figures, this is generally beyond the region of geophysical interest.

As a final remark, it is worth mentioning that higher-order terms in the density contrast, though more prone to computational noise as δ increases, provide a progressively lower contribute to gravity anomaly. This is in accordance with the significance of higher order density polynomials in 2D modelling. As a matter of fact geological settings require mostly 3D gravity modelling: the errors caused by 2D gravity modelling with high order polynomials will often be larger than the errors caused by piecewise constant densities in a relative few number of 3D polygonal bodies.

6 Conclusions

The gravity anomaly at arbitrary points produced by a 2D body whose shape is an arbitrary polygon and where density contrast varies with a polynomial law has been obtained in closed form. It is expressed as sum of quantities which depend only upon the coordinates of the vertices of the polygon and upon the parameters which define the density contrast. The solution procedure, based upon a generalized application of Gauss theorem, takes consistently into account the singularity intrinsic to the integrals to evaluate. Accordingly, by means of rigorous mathematical arguments, singularities are proved to give no contribution neither to the analytical expression of the gravity anomaly nor to its algebraic counterpart.

The formulation presented in the paper, which has been limited to polynomial density contrast varying with a cubic law as a maximum, can be easily extended to polynomials of higher degree. The effectiveness of the proposed approach has been intensively tested by numerical comparisons, carried out by means of a Matlab code, with several example derived from the specialized literature. Future contributions will concern the cases of density contrast variable with exponential law for 2D domains and 3D polyhedral bodies endowed with polynomial or exponential density contrasts.

7 Appendix A - Some useful differential identities

We prove hereafter some differential identities which are uesful for the derivations illustrated in the main body of the paper; they are reported in the same order in which they are required.

Let us begin with the component expression of the divergence of the rank-three tensor

$$\mathrm{div}[\psi(\mathbf{a}\otimes\mathbf{b}\otimes\mathbf{c})]_{ij} = \psi(\mathbf{a}_i\mathbf{b}_j\mathbf{c}_k)_{/k} \tag{117}$$

where $\mathbf{a}$, $\mathbf{b}$, $\mathbf{c}$ (ψ) are vector (scalar) differentiable fields and $(\cdot)_{/k}$ means derivation with respect to the k-th variable. Applying the chain rule to (117), Tang (2006), one obtains

$$\begin{aligned}\psi(\mathbf{a}_i\mathbf{b}_j\mathbf{c}_k)_{/k} &= \psi_{/k}\mathbf{a}_i\mathbf{b}_j\mathbf{c}_k + \psi\mathbf{a}_{i/k}\mathbf{b}_j\mathbf{c}_k + \psi\mathbf{a}_i\mathbf{b}_{j/k}\mathbf{c}_k + \psi\mathbf{a}_i\mathbf{b}_j\mathbf{c}_{k/k} = \\ &= (\mathbf{a}\otimes\mathbf{b}\otimes\mathbf{c})_{ijk}(\mathrm{grad}\psi)_k + \psi[(\mathrm{grad}\,\mathbf{a})\mathbf{c}]_i\mathbf{b}_j + \\ &\quad +\psi\mathbf{a}_i[(\mathrm{grad}\,\mathbf{b})\mathbf{c}]_j + \psi(\mathbf{a}\otimes\mathbf{b})_{ij}\mathrm{div}\,\mathbf{c}\end{aligned} \tag{118}$$

Thus, combining (117) and (118), one has

$$\begin{aligned}\mathrm{div}[\psi(\mathbf{a}\otimes\mathbf{b}\otimes\mathbf{c})] &= (\mathbf{a}\otimes\mathbf{b}\otimes\mathbf{c})\mathrm{grad}\,\psi + \psi[(\mathrm{grad}\,\mathbf{a})\mathbf{c}]\otimes\mathbf{b} + \\ &\quad +\psi\mathbf{a}\otimes[(\mathrm{grad}\,\mathbf{b})\mathbf{c}] + \psi(\mathbf{a}\otimes\mathbf{b})\mathrm{div}\,\mathbf{c}\end{aligned} \tag{119}$$

A further useful identity concerns the gradient of a scalar field expressed as scalar product of two vector fields

$$\mathrm{grad}\,(\mathbf{a}\cdot\mathbf{b}) = [\mathrm{grad}\,\mathbf{a}]^t\mathbf{b} + [\mathrm{grad}\,\mathbf{b}]^t\mathbf{a} \tag{120}$$

where $(\cdot)^t$ stands for transpose. It stems from the relation

$$[\mathrm{grad}\,(\mathbf{a}\cdot\mathbf{b})]_i = (\mathbf{a}_j\mathbf{b}_j)_{/i} \tag{121}$$

Actually, carrying out the derivations in the previous expression yields

$$(\mathbf{a}_j\mathbf{b}_j)_{/i} = \mathbf{a}_{j/i}\mathbf{b}_j + \mathbf{a}_j\mathbf{b}_{j/i} = [(\mathrm{grad}\,\mathbf{a})^t]_{ij}\mathbf{b}_j + [(\mathrm{grad}\,\mathbf{b})^t]_{ij}\mathbf{a}_j \tag{122}$$

which represents the component form of (120).

8 Appendix B - Recursive computation of integrals

Application of formula (56) requires the analytical computation of integrals of the kind

$$I_k = \int_0^1 \frac{x^k}{px^2 + 2qx + u} dx \tag{123}$$

where $p > 0$ and the discriminant of the denominator, i.e. $\Delta = q^2 - pu$, is assumed to be negative. Hence, the quadratic function $px^2 + 2qx + u$ is always positive on the real interval [0,1]. The case of a null discriminant Δ will be directly addressed in section 4 where the evaluation of I_{ki}, which makes use of the formulas derived hereafter for $\Delta < 0$, will be detailed.

As previously shown by Zhou (2010), the generic integral (123) can be computed recursively as function of two integrals, namely

$$I_0 = \int_0^1 \frac{1}{px^2 + 2qx + u} dx = \frac{1}{\sqrt{-\Delta}} \Big[\arctan \frac{p+q}{\sqrt{-\Delta}} - \arctan \frac{q}{\sqrt{-\Delta}} \Big] \tag{124}$$

and

$$I_1 = \int_0^1 \frac{x}{px^2 + 2qx + u} dx = \frac{1}{2p} \log \frac{p + 2q + u}{u} - \frac{q}{p} I_0 \tag{125}$$

Both results can be obtained, after some manipulation, by setting $t = x + q/p$ in the integrand functions above. To make the paper self-contained we rephrase the result in Zhou (2010)

$$J_k = \int \frac{x^k}{px^2 + 2qx + u} dx = \frac{x^{k-1}}{p(k-1)} - \frac{2q}{p} \int \frac{x^{k-1}}{px^2 + 2qx + u} dx - \frac{u}{p} \int \frac{x^{k-2}}{px^2 + 2qx + u} dx \tag{126}$$

where $k > 1$ and the terminology of this paper has been adopted.

For instance, if $k = 2$, one has

$$\begin{aligned} J_2 &= \int \frac{x^2}{px^2 + 2qx + u} dx = \frac{1}{p} \int \frac{px^2 + (2qx + u - 2qx - u)}{px^2 + 2qx + u} dx = \\ &= \frac{1}{p} \Big[\int dx - \int \frac{2qx + u}{px^2 + 2qx + u} dx \Big] = \\ &= \frac{1}{p} \Big[\int dx - 2q \int \frac{x}{px^2 + 2qx + u} dx - u \int \frac{dx}{px^2 + 2qx + u} \Big] = \\ &= \frac{1}{p} [x - 2qJ_1 - uJ_0] \end{aligned} \tag{127}$$

Analogously

$$J_3 = \frac{1}{p} \Big[\frac{x^2}{2} - 2qJ_2 - uJ_1 \Big] = \frac{1}{p} \Big[\frac{x^2}{2} - \frac{2qx}{p} + \frac{4q^2 - pu}{p} J_1 + \frac{2qu}{p} J_0 \Big] \tag{128}$$

and

$$J_4 = \frac{x^3}{3p} - \frac{q}{p^2} x^2 + \frac{4q^2 - pu}{p^3} x - \frac{2q(4q^2 - 2pu)}{p^3} J_1 - \frac{u(4q^2 - pu)}{p^3} J_0 \tag{129}$$

Hence

$$I_2 = \frac{1}{p}[1 - 2qI_1 - uI_0] \tag{130}$$

$$I_3 = \frac{1}{p}\Big[\frac{1}{2} - \frac{2q}{p} + \frac{4q^2 - pu}{p}I_1 + \frac{2qu}{p}I_0\Big] \tag{131}$$

and

$$I_4 = \frac{1}{p}\Big[\frac{1}{3} - \frac{q}{p} + \frac{4q^2 - pu}{p^2} - \frac{2q(4q^2 - 2pu)}{p^2}I_1 - \frac{u(4q^2 - pu)}{p^2}I_0\Big] \tag{132}$$

Acknowledgements The author wishes to express its deep gratitude to the Editor-in-Chief, prof. M.J. Rycroft, and to the three anonymous reviewers for careful suggestions and useful comments which resulted in an improved version of the original manuscript.

References

Aydemir A, Ates A, Bilim F, Buyuksarac A, Bektas O (2014) Evaluation of gravity and aeromagnetic anomalies for the deep structure and possibility of hydrocarbon potential of the region surrounding Lake Van, Eastern Anatolia, Turkey. Surv Geophys 35:431-448

Banerjee B, DasGupta SP (1977) Gravitational attraction of a rectangular parallelepiped. Geophysics 42:1053-1055

Barnett CT (1976) Theoretical modeling of the magnetic and gravitational fields of an arbitrarily shaped three-dimensional body. Geophysics 41:1353-1364

Bott MHP (1960) The use of rapid digital computing methods for direct gravity interpretation of sedimentary basins. Geophys J R Astr Soc 3:63-67

Cady JW (1980) Calculation of gravity and magnetic anomalies of finite length right polygonal prisms. Geophysics 45:1507-1512

Cai Y, Wang CY (2005) Fast finite-element calculation of gravity anomaly in complex geological regions. Geophys J Int 162:696-708

Chai Y, Hinze WJ (1988) Gravity inversion of an interface above which the density contrast varies exponentially with depth. Geophysics 53:837-845

Chakravarthi V, Raghuram HM, Singh SB (2002) 3-D forward gravity modeling of basement interfaces above which the density contrast varies continuously with depth. Comp & Geosc 28:53-57

Chakravarthi V, Sundararajan N (2007) 3D gravity inversion of basement relief: a depth-dependent density approach. Geophysics 72:I23-I32

Chappell A, Kusznir N (2008) An algorithm to calculate the gravity anomaly of sedimentary basins with exponential density-depth relationships. Geophys Prosp 56:249-258

Cordell L (1973) Gravity analysis using an exponential density depth function-San Jacinto graben, California. Geophysics 38:684-690

D'Urso MG, Russo P (2002) A new algorithm for point-in polygon test. Surv Rev 284:410-422

D'Urso MG (2012) New expressions of the gravitational potential and its derivates for the prism. In Hotine-Marussi International Symposium on Mathematical Geodesy, 7rd. Sneeuw N, Novák P, Crespi M, Sansò F. Springer-Verlag, Berlin Heidelberg pp. 251-256

D'Urso MG (2013a) On the evaluation of the gravity effects of polyhedral bodies and a consistent treatment of related singularities. J Geod 87:239-252

D'Urso MG, Marmo F (2013b) On a generalized Love's problem. Comp & Geosc 61:144-151

D'Urso MG (2014a) Analytical computation of gravity effects for polyhedral bodies. J Geod 88:13-29

D'Urso MG (2014b) Gravity effects of polyhedral bodies with linearly varying density. Cel Mech Dyn Astr 120:349-372

D'Urso MG, Marmo F (2015a) Vertical stress distribution in isotropic half-spaces due to surface vertical loadings acting over polygonal domains. Zeit Ang Math Mech 95:91-110

D'Urso MG (2015b) A remark on the computation of the gravitational potential of masses with linearly varying density. In Hotine-Marussi International Symposium on Mathematical Geodesy, 8rd. Sneeuw N, Novák P, Crespi M, Sansò F. Springer-Verlag, Berlin Heidelberg, in press

D'Urso, MG, Trotta S (2015c) Comparative assessment of linear and bilinear prism-based strategies for terrain correction computations. J Geod, doi: 10.1007/s00190-014-0770-4

Gallardo-Delgado LA, Pérez-Flores MA, Gómez-Treviño E (2003) A versatile algorithm for joint 3D inversion of gravity and magnetic data. Geophysics 68:949-959

García-Abdeslem J (1992) Gravitational attraction of a rectangular prism with depth dependent density. Geophysics 57:470-473

García-Abdeslem J (2005a) Gravitational attraction of a rectangular prism with density varying with depth following a cubic polynomial. Geophysics 70:J39-J42

García-Abdeslem J, Romo JM, Gómez-Treviño E, Ramírez-Hernández J, Esparza-Hernández FJ, Flores-Luna CF (2005b) A constrained 2D gravity model of the Sebastián Vizcaíno Basin, Baja California Sur, Mexico. Geophys Prosp 53:755-765

Gendzwill J (1970) The gradational density contrast as a gravity interpretation model. Geophysics 35:270-278

Golizdra GY (1981) Calculation of the gravitational field of a polyhedra. Izv Earth Phys (English Translation) 17:625-628

Götze HJ, Lahmeyer B (1988) Application of three-dimensional interactive modeling in gravity and magnetics. Geophysics 53:1096-1108

Guspí F (1990) General 2D gravity inversion with density contrast varying with depth. Geoexpl 26:253-265

Hamayun P, Prutkin I, Tenzer R (2009) The optimum expression for the gravitational potential of polyhedral bodies having a linearly varying density distribution. J Geod 83:1163-1170

Hansen RO (1999) An analytical expression for the gravity field of a polyhedral body with linearly varying density. Geophysics 64:75-77

Holstein H, Ketteridge B (1996) Gravimetric analysis of uniform polyhedra. Geophysics 61:357-364

Holstein H (2003) Gravimagnetic anomaly formulas for polyhedra of spatially linear media. Geophysics 68:157-167

Hubbert MK (1948) A line-integral method of computing the gravimetric effects of two-dimensional masses. Geophysics 13:215-225

Jacoby W, Smilde PL (2009) Gravity Interpretation - Fundamentals and Application of Gravity Inversion and Geological Interpretation. Springer, Berlin Heidelberg New York

Jiancheng H, Wenbin S (2010) Comparative study on two methods for calculating the gravitational potential of a prism. Geo-spat Inf Sci 13:60-64

Johnson LR, Litehiser JJ (1972) A method for computing the gravitational attraction of three dimensional bodies in a spherical or ellipsoinal earth. J Geoph Res 77:6999-7009

Kwok YK (1991a) Singularities in gravity computation for vertical cylinders and prisms. Geophys J Int 104:1-10

Kwok YK (1991b) Gravity gradient tensors due to a polyhedron with polygonal facets. Geophys Prosp 39:435-443

Li X, Chouteau M (1998) Three-dimensional gravity modelling in all spaces. Surv Geophys 19:339-368

Litinsky VA (1989) Concept of effective density: key to gravity depth determinations for sedimentary basins. Geophysics 54:1474-1482

Marmo F, Rosati L (2015) A general approach to the solution of Boussinesq's problem for polynomial pressures acting over polygonal domains. J Elast, submitted

Martín-Atienza B, García-Abdeslem J (1999) 2-D gravity modeling with analytically defined geometry and quadratic polynomial density functions. Geophysics 64:1730-1734

Montana CJ, Mickus KL, Peeples WJ (1992) Program to calculate the gravitational field and gravity gradient tensor resulting from a system of right rectangular prisms. Comp & Geosc 18:587-602

Mostafa ME (2008) Finite cube elements method for calculating gravity anomaly and structural index of solid and fractal bodies with defined boundaries. Geophys J Int 172:887-902

Murthy IVR, Rao DB (1979) Gravity anomalies of two-dimensional bodies of irregular cross-section with density contrast varying with depth. Geophysics 44:1525-1530

Murthy IVR, Rao DB, Ramakrishna P (1989) Gravity anomalies of three dimensional bodies with a variable density contrast. Pure Appl Geophysics 30:711-719

Nagy D (1966) The gravitational attraction of a right rectangular prism. Geophysics 31:362-371

Nagy D, Papp G, Benedek J (2000) The gravitational potential and its derivatives for the prism. J Geod 74:553-560

Okabe M (1979) Analytical expressions for gravity anomalies due to homogeneous polyhedral bodies and translation into magnetic anomalies. Geophysics 44:730-741

Pan JJ (1989) Gravity anomalies of irregularly shaped two-dimensional bodies with constant horizontal density gradient. Geophysics 54:528-530

Paul MK (1974) The gravity effect of a homogeneous polyhedron for three-dimensional interpretation. Pure Appl Geophys 112:553-561

Petrović S (1996) Determination of the potential of homogeneous polyhedral bodies using line integrals. J Geod 71:44-52

Plouff D (1975) Derivation of formulas and FORTRAN programs to compute gravity anomalies of prisms. Nat Tech Inf Serv No PB-243-526. US Dept of Commerce, Springfield, VA

Plouff D (1976) Gravity and magnetic fields of polygonal prisms and application to magnetic terrain corrections. Geophysics 41:727-741

Pohanka V (1988) Optimum expression for computation of the gravity field of a homogeneous polyhedral body. Geophys Prospect 36:733-751

Pohanka V (1998) Optimum expression for computation of the gravity field of a polyhedral body with linearly increasing density. Geophys Prospect 46:391-404

Rao DB (1985) Analysis of gravity anomalies over an inclined fault with quadratic density function. Pageoph 123:250-260

Rao DB (1986) Modeling of sedimentary basins from gravity anomalies with variable density contrast. Geophys J R Astr Soc 84:207-212

Rao DB (1990) Analysis of gravity anomalies of sedimentary basins by an asymmetrical trapezoidal model with quadratic function. Geophysics 55:226-231

Rao DB, Prakash M J, Babu R N (1990) 3D and 2 1/2 modeling of gravity anomalies with variable density contrast. Geophys Prosp 38:411-422

Rao CV, Chakravarthi V, Raju ML (1994) Forward modelling: gravity anomalies of two-dimensional bodies of arbitrary shape with hyperbolic and parabolic density functions. Comp & Geosc 20:873-880

Rosati L, Marmo F (2014) Closed-form expressions of the thermo-mechanical fields induced by a uniform heat source acting over an isotropic half-space. Int J Heat Mass Transfer 75:272-283

Ruotoistenmäki T (1992) The gravity anomaly of two-dimensional sources with continuous density distribution and bounded by continuous surfaces. Geophysics 57:623-628

Sessa S, D'Urso MG (2013) Employment of Bayesian networks for risk assessment of excavation processes in dense urban areas. Proc 11th Int Conf ICOSSAR 2013, 30163-30169

Silva JB, Costa DCL, Barbosa VCF (2006) Gravity inversion of basement relief and estimation of density contrast variation with depth. Geophysics 71:J51-J58

Strakhov VN (1978) Use of the methods of the theory of functions of a complex variable in the solution of three-dimensional direct problems of gravimetry and magnetometry. Dokl Akad Nauk 243:70-73

Strakhov VN, Lapina MI, Yefimov AB (1986) A solution to forward problems in gravity and magnetism with new analytical expression for the field elements of standard approximating body. Izv Earth Phys (English Translation) 22:471-482

Talwani M, Worzel JL, Landisman M (1959) Rapid gravity computations for two-dimensional bodies with application to the Mendocino submarine fracture zone. J Geophys Res 64:49-59

Tang KT (2006) Mathematical Methods for Engineers and Scientists. Springer, Berlin Heidelberg New York

Tenzer R, Novák P, Vajda P, Gladkikh V, Hamayun (2012) Spectral harmonic analysis and synthesis of Earth's crust gravity field. Comp & Geosc 16: 193-207

Tenzer R, Gladkikh V, Vajda P, Novák P (2012) Spatial and spectral analysis of refined gravity data for modelling the crust-mantle interface and mantle-lithosphere structure. Surv Geophys 33: 817-839

Tenzer R, Novák P, Hamayun, Vajda P (2012) Spectral expressions for modelling the gravitational field of the Earth's crust density structure. Stud Geoph Geod 56: 141-152

Tsoulis D (2000) A note on the gravitational field of the right rectangular prism. Boll Geod Sc Aff LIX-1:21-35

Tsoulis D, Petrović S (2001) On the singularities of the gravity field of a homogeneous polyhedral body. Geophysics 66:535-539

Tsoulis D (2012) Analytical computation of the full gravity tensor of a homogeneous arbitrarily shaped polyhedral source using line integrals. Geophysics 77:F1-F11

Waldvogel J (1979) The Newtonian potential of homogeneous polyhedra, J Appl Math Phys 30:388-398

Werner RA (1994) The gravitational potential of a homogeneous polyhedron. Celest Mech Dynam Astr 59:253-278

Werner RA, Scheeres DJ (1997) Exterior gravitation of a polyhedron derived and compared with harmonic and mascon gravitation representations of asteroid 4769 Castalia. Celest Mech Dynam Astr 65:313-344

Won IJ, Bevis M (1987) Computing the gravitational and magnetic anomalies due to a polygon: algorithms and Fortran subroutines. Geophysics 52:232-238

Zhang J, Zhong B, Zhou X, Dai Y (2001) Gravity anomalies of 2D bodies with variable density contrast. Geophysics 66:809-813

Zhou X (2008) 2D vector gravity potential and line integrals for the gravity anomaly caused by a 2D mass of depth-dependent density contrast. Geophysics 73:I43-I50

Zhou X (2009a) General line integrals for gravity anomalies of irregular 2D masses with horizontally and vertically dependent density contrast. Geophysics 74:I1-I7

Zhou X (2009b) 3D vector gravity potential and line integrals for the gravity anomaly of a rectangular prism with 3D variable density contrast. Geophysics 74:I43-I53

Zhou X (2010) Analytical solution of gravity anomaly of irregular 2D masses with density contrast varying as a 2D polynomial function. Geophysics 75:I11-I19

Answer to the Managing Editor

prof. Michael J. Rycroft

Dear prof. Rycroft,

please find enclosed the revised version of the paper GEOP-D-14-00056R1:

The gravity anomaly of a 2D polygonal body having density contrast given by polynomial functions
by
M.G. DõUrso

which I have submitted for publication on Surveys in Geophysics.

First of all let me thank You once more for your useful comments which have been properly acknowledged at the end of the revised version of the manuscript.

Responses to the comments made by reviewers are attached to this letter in three separate files. In particular, as requested by reviewer #3, I have added the word ñ2Dò to the title of the paper.

Waiting from Your please receive my best regards and best wishes of a Happy New Year.

Cassino, January 3rd 2015 Maria Grazia DõUrso

Answer to reviewer # 1

The author wishes to thank the reviewer for careful reading of the original manuscript and useful comments which have been properly acknowledged at the end of the revised version of the manuscript.

According to the comments pointed out by the reviewer, the original manuscript has been modified as follows:

Abstract

Remark 0.1:
"The solution presented in the paper refers to a third-order polynomial function although its expression exhibits an intrinsic symmetry ..."
Why "although"?

The sentence has been changed as follows: The solution presented in the paper, which refers to a third-order polynomial function as a maximum, exhibits an intrinsic symmetry which naturally suggests its extension to the case of higher-order polynomials describing the density contrast.

1 Introduction:

Remark 1.1:
"The gravity anomaly of a region represents a fundamental set of geophysical data..."
"For this reason it is extremely beneficial to dispose of analytical solutions..."
Although gravity modelling is my main interest too, I nevertheless find the words "fundamental" and "extremely" somewhat exaggerated.

The word ñfundamentalò has been changed to ñbasicò and the word ñextremelyò to ñhighlyò.

Remark 1.2:
"... simple geometric modelling, i.e. the use of prisms, and refined modelling of the density contrast. A converse approach is based on the use of polyhedra ..."
Instead of the unsuitable binary classification "converse", I would suggest "different" or possibly "alternative".

The word ñdifferentò has been used.

2 Gravity anomaly of a 2D body at the origin O of the reference frame

Remark 2.1:
In the gravity literature the letter rho usually designates density. In eq. 6, however, it represents distance. On the other hand, eq. 4 designates density by the letter delta, which is usually related to some type of differences, especially in integrals as they are occurring abundantly in this paper. Using a more common selection of variable letters would improve the readability of this paper.

The whole notation has been changed. Namely the density contrast has been initially denoted as $\Delta\rho$ and subsequently with the more concise letter θ. The coefficients of the polynomial expression of the density contrast have been denoted by **c**, **C** and ***C*** (I donôt have in Word the right symbol as in LaTeX). Analogously, the tensor products of ρ have been denoted by **d**, **D** and ***D***. I have not changed the symbol ρ to designate the position vector since I have already used it in all my papers. On the other hand it is written in boldface so that there should not be any confusion with $\Delta\rho$ used only at the beginning of the paper.

Remark 2.1:
In eq. 7 the letter g, designating gravity in eq. 6, is confusingly reused for linear polynomial coefficients of density.

The symbol **c** has been used in place of the misleading **g**.

Remark 2.2:
I assume, in eq. 15 it should read "... = 1/3 a21" and "... = 1/3 a12".

You are right. Correction has been made.

Remark 2.3:
In eq. 17 (and later) it is difficult to discriminate (optically) between the scalar (normal face) iota and the vector (bold) iota.

The scalar (normal face) iota has been left while the vector (bold) iota has been changed to κ.

Remark 2.4:
I would prefer a more consistent naming of the left hand sides of eq.s 17 and 18. Iota for both (!) rank 0 and 1 tensors, A for rank 2 and B for 3 tensors is slightly confusing again.

I have changed the symbols to *d*, **d**, **D** and ***D***.

4 Ineffective singularities of the algebraic expressions of the gravity anomaly

Remark 4.1:
As far as I know, Newton's gravity equation (eq. 3) is already known to be singularity-free for singularity-free/finite density distributions, calculated anywhere in space. So, if you show that your formulation is singularity-free, aren't you mainly showing that your formulation is merely behaving as expected?

This is only partially true in the sense that, as You correctly state, Newtonõs gravity equation is already known to be singularity-free for singularity-free/finite density distributions. The problem of singularity arises with the algebraic counterparts of Newtonõs integral. Previous authors did not succeed in rigorously eliminating the singularity from their formulas if not artificially moving aside the observation point by an infinitesimal quantity. Thatõs why I named the section ñIneffective singularities of the *ALGEBRAIC* expressions of the gravity anomalyò.

Remark 4.2:
Most (good) calculations schemes for polyhedra (2D as well as 3D) that I know can be calculated at any position in space except at the vertices and/or at the edges. In all these cases it also suffices to skip the calculation at these vertices/edges. Thus, from the computational point of view, it would be most interesting to arrive at a formulation, where it wouldn't even be necessary to skip these vertices/edges.

This is actually what has been made in the paper. Calculations are not skipped at vertices/edges since they can be made for every position of the observation point; as shown in subsections 4.1-4.3, I only need to suitably specialize the general formulas.

5 Numerical examples:

Remark 5.1:
Are there any explanations for systematic differences between the reference results and your ones (fig. 4 left side yours higher, right side yours lower; fig. 8 (Zhou 2008) left side yours lower, right side equal, fig. 10 left side yours lower, right side equal, fig. 12 left side yours higher, right side yours lower).

No, I could not find any reasonable explanation. In any case I am sure about the correctness of my results since I computed the integrals also numerically

6 Conclusions:

Remark 6.1:
Interesting and important would be a discussion about the accuracy of the present solution method in the context of distance-to-body vs. size-of-body as preformed in many papers of Holstein et al. in the past years. Please extend your paper.

Subsection 5.1 ñError analysisò has been added to the revised version of the manuscript

Remark 6.2:
Another important fact to consider is the significance of high(er) order density polynomials in 2D modelling. Geological settings require mostly 3D gravity modellings; the errors caused by 2D gravity modelling with high order polynomials will often be larger then the errors caused by (piecewise) constant densities in a relative (sic!) few number of 3D polygonal bodies.

Considerations on this issue has been added at pag. 26, at the end of subsection 5.1 .

Answer to reviewer # 2

The author wishes to thank the reviewer for careful reading of the original manuscript and useful comments which have been properly acknowledged at the end of the revised version of the manuscript.

According to the comments pointed out by the reviewer, the original manuscript has been modified as follows:

Eq. (3) defines "gravitation" not "gravity attraction"

Correction has been made, see line before formula (1) of the revised version of the manuscript.

Eq. (4) defined vertical component of gravitation

Correction has been made, see line before formula (2) of the revised version of the manuscript

I do not really know what is the "gravity anomaly" Is that the gravitation generated by the density contrast interface? Please explain clearly.

It has been done soon after formula (3) of the revised version of the manuscript.

In Eq. (31) the meaning of index n is not clear, please clarify that it represents the number of edges in the polygon (see Fig. 1)

The meaning of *n* had been already specified in the line before formula (31); in any case, I have added reference to Fig. 1 before formula (32) of the revised version of the manuscript.

It might be useful to number the equations in Appendices separately from the main text, i.e. (A.1), (A.2), ***é***

I agree with You but the paper has been prepared by using the LaTeX class file of the journal; hence, I cannot modify the original settings concerning numbering of equations.

In the numerical test I am missing the comparison of the CPU which is required for the computation using different methods. Such a comparison would be useful for users when dealing with more *complex numerical tasks, taking the computational time into consideration.*

I have added the CPU time to the caption of the tables which have been included in the revised version of the paper to meet the request of another reviewer.

Tenzer et al. (2012) developed spectral expressions for computing the gravitational effect of an arbitrary volumetric mass layers while assuming the laterally varying radial density changes; see
Tenzer R, NovÃ¡k P, Vajda P, Gladkikh V, Hamayun (2012) Spectral harmonic analysis and synthesis of Earth's crust gravity field. Computational Geosciences 16(1): 193-207
Tenzer R, Gladkikh V, Vajda P, NovÃ¡k P (2012) Spatial and spectral analysis of refined gravity data for modelling the crust-mantle interface and mantle-lithosphere structure. Surv Geophys 33(5): 817-839
Tenzer R, NovÃ¡k P, Hamayun, Vajda P (2012) Spectral expressions for modelling the gravitational field of the Earth's crust density structure. Stud Geoph Geod 56(1): 141-152

Reference to these more refined computations have been added at the beginning of pag. 20, soon after Table 1.

Answer to Reviewer #3

The author wishes to thank the reviewer for careful reading of the original manuscript and useful comments which have been properly acknowledged at the end of the revised version of the manuscript.
According to the comments pointed out by the reviewer, the original manuscript has been modified as follows:

1. *I believe that the reference to 2D-sources should be explicitly included in the paper's title. I understand that the term 'polygonal' is used from the author exactly for this purpose; however, there also exist polygonal lines, which express 1D distributions. In any case, I feel that the title could be somehow polished up in this direction.*

   The word ñ2Dò has been added to the title.

2. *Figures 4, 6, 8, 10 and 12 should be accompanied with the numerical information regarding the corresponding differences. The values themselves are great, but when comparing to other formulas it would be helpful to get an impression of the differences, which right now are not visible. Graphically this would probably be difficult, perhaps in terms of a subplot with logarithmic scale (the dots seem to almost coincide with existing approaches). Or in terms of table(s) with statistics of the differences, or/and finally as a detailed inline textual information. This addition will make more clear whether the 'present approach' produces variations that have only to do with the internal accuracy level of the computer or whether it defines real numerical differences against existing methods.*

   Tables 1-5 have been added to the revised version of the manuscript. In the captions I have specified that results from other sources in the literature have been simply inferred from the figures in which they have been originally reported.